

Measurement of $W^\pm Z$ production in proton-proton collisions at $\sqrt{s} = 7$ TeV with the ATLAS detector

The ATLAS Collaboration*

CERN, 1211 Geneva 23, Switzerland

Received: 7 August 2012 / Revised: 14 September 2012 / Published online: 6 October 2012

© CERN for the benefit of the ATLAS collaboration 2012. This article is published with open access at Springerlink.com

Abstract A study of $W^\pm Z$ production in proton-proton collisions at $\sqrt{s} = 7$ TeV is presented using data corresponding to an integrated luminosity of 4.6 fb^{-1} collected with the ATLAS detector at the Large Hadron Collider in 2011. In total, 317 candidates, with a background expectation of 68 ± 10 events, are observed in double-leptonic decay final states with electrons, muons and missing transverse momentum. The total cross-section is determined to be $\sigma_{WZ}^{\text{tot}} = 19.0^{+1.4}_{-1.3}(\text{stat.}) \pm 0.9(\text{syst.}) \pm 0.4(\text{lumi.}) \text{ pb}$, consistent with the Standard Model expectation of $17.6^{+1.1}_{-1.0} \text{ pb}$. Limits on anomalous triple gauge boson couplings are derived using the transverse momentum spectrum of Z bosons in the selected events. The cross-section is also presented as a function of Z boson transverse momentum and diboson invariant mass.

1 Introduction

The underlying structure of electroweak interactions in the Standard Model (SM) is the non-abelian $SU(2)_L \times U(1)_Y$ gauge group. This model has been very successful in describing measurements to date. Properties of electroweak gauge bosons such as their masses and couplings to fermions have been precisely measured at LEP, the Tevatron and SLD [1]. However, triple gauge boson couplings (TGCs) predicted by this theory have not yet been determined with a similar precision.

In the SM, the TGC vertex is completely determined by the electroweak gauge structure and so a precise measurement of this vertex, for example through the analysis of diboson production at the Large Hadron Collider (LHC), tests the gauge symmetry and probes for possible new phenomena involving gauge bosons. Anomalous TGCs, deviating from gauge constraints, may enhance the $W^\pm Z$ production

cross-section at high diboson invariant masses. The cross-section can also be enhanced by the production of new particles decaying into $W^\pm Z$ pairs, such as those predicted in supersymmetric models with an extended Higgs sector and models with extra vector bosons [2].

At the LHC, $W^\pm Z$ diboson production arises predominantly from quark-antiquark initial states at leading order (LO) and quark-gluon initial states at next-to-leading order (NLO) [3]. Figure 1 shows the LO Feynman diagrams for $W^\pm Z$ production from $q\bar{q}'$ initial states. Only the s -channel diagram has a TGC vertex and is hence the only channel to contribute to potential anomalous coupling behaviour of gauge bosons.

In proton-proton (pp) collisions at a centre-of-mass energy $\sqrt{s} = 7$ TeV, the SM cross-section for $W^\pm Z$ production is predicted at NLO to be $17.6^{+1.1}_{-1.0} \text{ pb}$. This has been computed for $66 < m_{\ell\ell} < 116 \text{ GeV}$, where $m_{\ell\ell}$ is the invariant mass of the dilepton system from the Z boson decay, using MCFM [4] with the CT10 [5] parton distribution functions (PDFs). The uncertainty on the prediction comes from the PDF uncertainties, evaluated using the CT10 eigenvector sets, and the QCD renormalization and factorization scales, which are varied simultaneously up or down by a factor of two with respect to the nominal value of $(m_W + m_Z)/2$.

This paper presents measurements of the $W^\pm Z$ production cross-section with the ATLAS detector in pp collisions at $\sqrt{s} = 7$ TeV. The analysis considers four channels of double-leptonic decays $W^\pm Z \rightarrow \ell^\pm \nu \ell^\pm \ell^-$ involving electrons and muons, i.e. $e^\pm e^+ e^-$, $\mu^\pm e^+ e^-$, $e^\pm \mu^+ \mu^-$ and $\mu^\pm \mu^+ \mu^-$, plus large missing transverse momentum. The results are based on an integrated luminosity of $4.64 \pm 0.08 \text{ fb}^{-1}$ collected in 2011, and supersede the earlier ATLAS results based on a subsample of these data [6].

The paper is organized as follows: Sect. 2 briefly describes the ATLAS detector and the data sample, including the simulated signal and background samples used in this analysis. Section 3 details the definition and reconstruction of physically observable objects such as particles and

* e-mail: atlas.publications@cern.ch

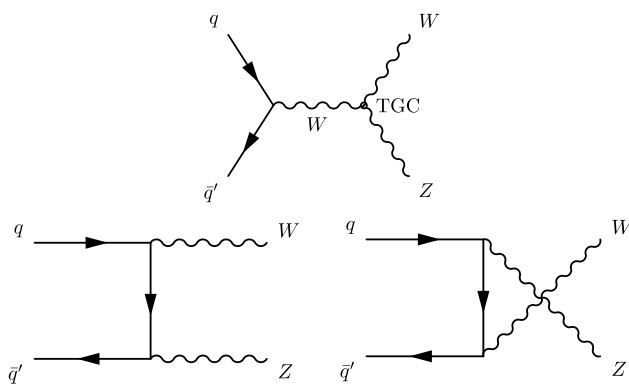


Fig. 1 The SM tree-level Feynman diagrams for $W^\pm Z$ production through the s -, t -, and u -channel exchanges in $q\bar{q}'$ interactions at hadron colliders

jets, and the event selection criteria. Section 4 presents the signal acceptance, and Sect. 5 the background estimation. Section 6 presents the measured $W^\pm Z$ production cross-section, constraints on the anomalous TGCs, and the fiducial cross-section as a function of the Z boson transverse momentum and the $W^\pm Z$ diboson invariant mass.

2 The ATLAS detector and data sample

The ATLAS detector [7] is a multi-purpose particle physics detector operating at one of the beam interaction points of the LHC.¹ The innermost part of the detector is a precision tracking system covering the pseudorapidity range $|\eta| < 2.5$. It consists of silicon pixels, silicon strips, and straw-tube chambers operating in a 2 T axial magnetic field supplied by a superconducting solenoid. Outside the solenoid are highly segmented electromagnetic and hadronic calorimeters covering $|\eta| < 4.9$.

The outermost subsystem is a large muon spectrometer covering $|\eta| < 2.7$, which reconstructs muon tracks and measures their momenta using the azimuthal magnetic field produced by three sets of air-core superconducting toroids. This analysis primarily uses the inner detector and the electromagnetic calorimeter to reconstruct electrons, the inner detector and the muon spectrometer to reconstruct muons, and the electromagnetic and hadronic calorimeters to reconstruct the missing momentum transverse to the beam line, E_T^{miss} . The E_T^{miss} is corrected to account for muons reconstructed by the inner detector and the muon spectrometer.

¹ATLAS uses a right-handed coordinate system with its origin at the nominal interaction point (IP) in the centre of the detector and the z -axis along the beam pipe. The x -axis points from the IP to the centre of the LHC ring, and the y -axis points upward. Cylindrical coordinates (r, ϕ) are used in the transverse plane, ϕ being the azimuthal angle around the beam pipe. The pseudorapidity is defined in terms of the polar angle θ as $\eta = -\ln \tan(\theta/2)$.

$W^\pm Z$ candidate events with multi-lepton final states are selected with single-muon or single-electron triggers. During the 2011 data-taking, the transverse momentum (p_T) threshold for the single-muon trigger was 18 GeV. The p_T threshold for the single-electron trigger was initially 20 GeV, and was raised to 22 GeV in the latter part of 2011 to cope with increasing instantaneous luminosity. For the $W^\pm Z$ events that pass all selection criteria, the trigger efficiency is in the range of (96–99) % depending on the final state being considered.

2.1 Simulated event samples

Simulated event samples are used to estimate both the signal selection efficiency and some of the background contributions. The response of the ATLAS detector is simulated [8] using GEANT4 [9].

The production of $W^\pm Z$ pairs and subsequent decays are modelled with the MC@NLO [10, 11] event generator, which incorporates NLO QCD matrix elements into the parton shower by interfacing to the HERWIG [12] program. The CT10 [5] PDF set is used. The underlying event is modelled with the JIMMY [13] program.

Background processes for $W^\pm Z$ signal detection are jets produced in association with W^\pm or Z bosons, W^+W^- and ZZ pairs, and top-quark production events. ALPGEN [14] is used to model the $W^\pm/Z + \text{jets}$ and Drell-Yan processes for W^\pm/Z bosons decaying to e , μ and τ leptons. Events with multi-jet production from heavy-flavour partons are modelled with PYTHIA8 [15]. The W^+W^- and ZZ processes are modelled with HERWIG and PYTHIA [16], respectively. The $W^\pm/Z + \gamma$ and $t\bar{t} + W^\pm/Z$ processes are produced with MADGRAPH [17]. The $t\bar{t}$ and single top-quark events are modelled with MC@NLO. Whenever LO event generators are used, the cross-sections are corrected to NLO or, if available, NNLO matrix element calculations [10, 18–23].

HERWIG is used to model the hadronization, initial-state radiation and QCD final-state radiation (FSR), except for the samples generated with PYTHIA or MADGRAPH, for which PYTHIA is used. PHOTOS [24] is used for QED FSR, and TAUOLA [25] for the τ lepton decays.

Each simulated sample is divided into subsamples that reflect the changes in the data-taking conditions in 2011. The average number of interactions per bunch crossing, $\langle \mu \rangle$, increased throughout 2011 with the instantaneous luminosity, and reached a maximum of 17. Particles produced in multiple interactions, either coincident with the event of interest or in neighbouring bunch crossings, are referred to as ‘pile-up’ and are included in the simulation. The number of extra interactions in simulated events is adjusted according to the measured $\langle \mu \rangle$ distribution in each data-taking period.

3 Event reconstruction and selection

The following event selection criteria are applied to the events collected with the single-electron or single-muon trigger described in Sect. 2. A primary vertex reconstructed from at least three well-reconstructed charged-particle tracks, each with $p_T > 400$ MeV, is required in order to remove non-collision background and ensure good object reconstruction. If an event contains more than one primary vertex, the vertex with the largest total p_T^2 of the associated tracks is selected.

3.1 Object reconstruction and selection

Events are selected in the $W^\pm Z \rightarrow \ell^\pm \nu \ell^\pm \ell^-$ channel, where the ℓ are either e or μ . The physical objects selected are electrons, muons, and neutrinos that manifest themselves as E_T^{miss} . Contamination from jets, mainly due to semileptonic decays of hadrons or due to misidentification of hadrons as leptons, is suppressed by requiring the electrons and muons to be isolated from other reconstructed objects.

Muon candidates are identified by matching tracks reconstructed in the muon spectrometer to tracks reconstructed in the inner detector. The momentum of the *combined* muon track is calculated from the momenta of the two tracks corrected for the energy loss in the calorimeter. To identify muons that traverse fewer than two of the three layers of the muon spectrometer, inner detector tracks that match at least one track segment in the muon spectrometer are also included. Such muons are referred to as *tagged* muons to distinguish them from the combined muons. The transverse momentum of the muon must be greater than 15 GeV and the pseudorapidity $|\eta| < 2.5$, using the full range of the inner detector. The muon momentum in simulated events is smeared to account for a small difference in resolution between data and simulation. At the closest approach to the primary vertex, the ratio of the transverse impact parameter d_0 to its uncertainty (the d_0 significance) must be smaller than three, and the longitudinal impact parameter $|z_0|$ must be less than 1 mm. These requirements reduce contamination from heavy flavour decays. Isolated muons are selected with a requirement that the scalar sum of the p_T of the tracks within $\Delta R = 0.3$ of the muon, where $\Delta R \equiv \sqrt{(\Delta\eta)^2 + (\Delta\phi)^2}$, must be less than 15 % of the muon p_T .

Electron candidates are formed by matching clusters found in the electromagnetic calorimeter to tracks reconstructed in the inner detector [26]. The transverse energy E_T , calculated from the cluster energy and the track direction, must be greater than 15 GeV. The pseudorapidity of the cluster must be in the ranges $|\eta| < 1.37$ or $1.52 < |\eta| < 2.47$ to ensure good containment of the electromagnetic shower in the calorimeters. The lateral and transverse shapes of the

cluster must be consistent with those of an electromagnetic shower. The d_0 significance must be smaller than 10, and $|z_0|$ must be less than 1 mm. To ensure isolation, the total calorimeter E_T in a cone of $\Delta R = 0.3$ around the electron candidate, not including the E_T of the candidate itself, must be less than 14 % of the electron E_T , and the scalar sum of the p_T of the tracks within $\Delta R = 0.3$ of the electron must be less than 13 % of the electron p_T . The calorimeter response is corrected for the additional energy deposited by pile-up. The electron energy in simulated events is smeared to account for a small difference in resolution between data and simulation. If an electron candidate and a muon candidate are found within $\Delta R = 0.1$ of each other, the electron candidate is removed. This mainly removes final-state radiation, where a photon was misidentified as an electron, and also jets from pile-up that were misidentified as electrons.

The missing transverse momentum E_T^{miss} is estimated from reconstructed electrons with $|\eta| < 2.47$, muons with $|\eta| < 2.7$, jets with $|\eta| < 4.9$, as well as clusters of energy in the calorimeter not included in reconstructed objects with $|\eta| < 4.5$ [27]. The clusters are calibrated to the electromagnetic or the hadronic energy scale according to cluster topology. The expected energy deposit of the muon in the calorimeter is subtracted. Jets are reconstructed with the anti- k_t jet-finding algorithm [28] with radius parameter $R = 0.4$, and are calibrated and corrected for detector effects using simulation, which has been tuned and validated with data. Events that contain jets, with $p_T > 20$ GeV and $|\eta| < 4.9$, which are poorly reconstructed as determined using calorimeter signal timing and shower shape information, are rejected to improve E_T^{miss} resolution.

3.2 Signal event selection

Events with two leptons of the same flavour and opposite charge with an invariant mass $m_{\ell\ell}$ within 10 GeV of the Z boson mass are selected. This reduces much of the background from multi-jet, top-quark, and W^+W^- production. Figure 2(a) shows the $m_{\ell\ell}$ distribution of the Z candidate in events that pass the complete event selection criteria described in this section, except for the $m_{\ell\ell}$ requirement.

Events are then required to have at least three reconstructed leptons originating from the same primary vertex, two leptons from a Z boson decay and one additional lepton attributed to the decay of a W^\pm boson. To reduce background from $Z +$ jets, the third lepton is required to pass more stringent identification criteria than required for the leptons attributed to the Z boson. The additional criteria imposed on electrons are: a more stringent quality requirement for the matched track, a requirement on the ratio of the energy measured in the calorimeter to the momentum of the matched track, and a requirement that transition radiation is detected if the candidate traversed the straw-tube chambers.

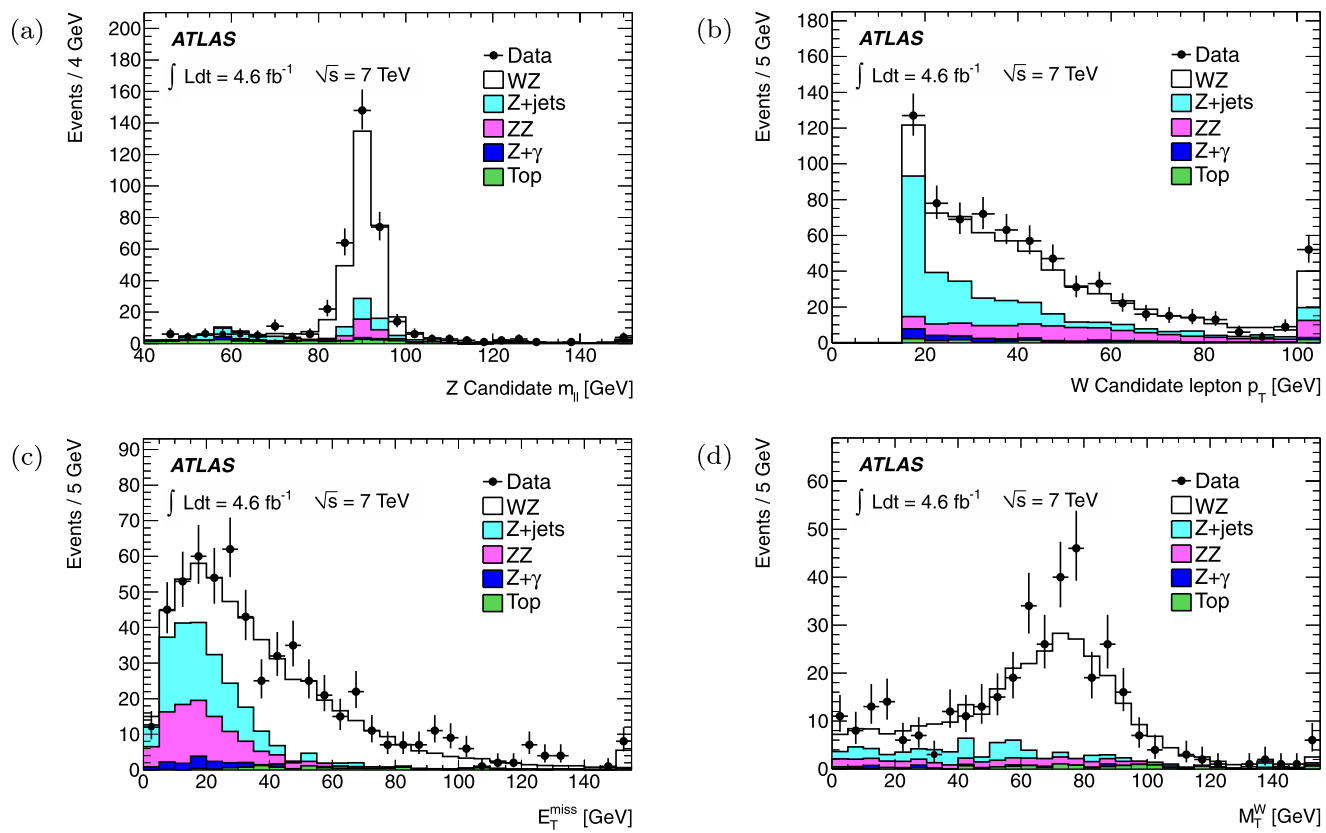


Fig. 2 (a) Dilepton invariant mass m_{ll} of the Z candidate in the events that pass all event selection criteria except for the m_{ll} cut. (b) Transverse momentum p_T of the lepton attributed to the W candidate. (c) Missing transverse momentum E_T^{miss} of the trilepton events. (d) Transverse mass M_T^W of the W candidates. Samples shown in (b),

(c), and (d) are the candidate events remaining before the cut on the variable displayed. The stacked histograms are expectations from simulation for WZ , ZZ , and $Z + \gamma$. For $Z + \text{jets}$ and $t\bar{t}$, the expected shape is taken from simulation but the normalization is taken from the data-driven estimates. The rightmost bins include overflows

Muons attributed to the W^\pm boson decay are required to be reconstructed as combined, and not tagged, muons. Figure 2(b) shows the p_T distribution of the third leptons that pass the additional identification criteria. The third lepton is required to have $p_T > 20$ GeV.

Figure 2(c) shows the E_T^{miss} distribution of the selected trilepton events. The events have to satisfy $E_T^{\text{miss}} > 25$ GeV.

The transverse mass of the W^\pm boson is calculated as

$$M_T^W = \sqrt{2p_T^\ell E_T^{\text{miss}}(1 - \cos(\Delta\phi))}, \quad (1)$$

where p_T^ℓ is the transverse momentum of the third lepton and $\Delta\phi$ is the azimuthal angle between the third lepton and the E_T^{miss} . Figure 2(d) shows the M_T^W distribution of the events that reach this stage of the selection. The observed M_T^W distribution appears to have a narrower peak than predicted by the simulation. The events with $70 < M_T^W < 80$ GeV have been scrutinized for signs of experimental problems, and no issues were found. The limited resolution of the E_T^{miss} measurement makes it unlikely that the observed excess is a narrow peak.

M_T^W is required to be greater than 20 GeV. The E_T^{miss} and M_T^W requirements suppress most of the remaining background from $Z + \text{jets}$ and other diboson production.

In order to ensure that the trigger efficiency is well determined, at least one of the muons (electrons) from the $W^\pm Z$ candidate is required to have $p_T > 20$ (25) GeV and to be geometrically matched to a muon (electron) reconstructed by the trigger algorithm. These p_T thresholds are sufficiently large compared with the trigger p_T thresholds to guarantee that the efficiency is not dependent on the p_T of the lepton.

4 Signal acceptance

The numbers of simulated $W^\pm Z$ events after each stage of the event selection, scaled to 4.6 fb^{-1} , are listed in Table 1. The “Efficiency corrections” row shows the predictions corrected for the differences in the trigger and reconstruction efficiencies between the measured and simulated data. The acceptance increases with the number of muons in the final state because the reconstruction efficiency for muons is

higher than for electrons. The additional contribution from $W^\pm Z \rightarrow \tau + X$, where the τ decays into an electron or a muon, is shown in the last row of Table 1.

Table 2 summarizes the systematic uncertainties on the expected signal yields. For electrons and muons, the reconstruction efficiencies, p_T scale and resolution, and efficiencies for the isolation and impact-parameter requirements are studied using samples of W^\pm , Z , and J/ψ decays. Differ-

Table 1 Expected number of signal $W^\pm Z \rightarrow \ell^\pm \nu \ell^\pm \ell^-$ events after each stage of selection. The first nine rows are computed with a simulated $W^\pm Z$ sample scaled to 4.6 fb^{-1} . Efficiency corrections refer to application of correction factors that account for the differences in the trigger and reconstruction efficiencies between the real and simulated data. The last row shows the additional contribution from $W^\pm Z \rightarrow \tau + X$

	eee	μee	$e\mu\mu$	$\mu\mu\mu$
Generated		1202		
Muon or electron trigger		1121		
Primary vertex		1118		
Jet cleaning		1116		
Two leptons, $m_{\ell\ell}$	219		317	
Three leptons, p_T	51.2	70.6	74.8	106.6
$E_T^{\text{miss}} > 25 \text{ GeV}$	40.5	57.0	59.2	86.4
$M_T^W > 20 \text{ GeV}$	38.1	54.1	55.7	81.9
Trigger match	38.0	54.0	55.3	81.7
Efficiency corrections	37.2	51.8	54.2	78.3
$W^\pm Z \rightarrow \tau X$ contribution	1.7	2.3	2.4	3.4

Table 2 Systematic uncertainties, in %, on the expected signal yields

Source	eee	μee	$e\mu\mu$	$\mu\mu\mu$
μ reconstruction efficiency	–	0.3	0.5	0.8
μ p_T scale & resolution	–	< 0.1	0.1	0.1
μ isolation & impact param.	–	0.2	0.4	0.6
e reconstruction efficiency	2.5	1.7	0.8	–
e identification efficiency	3.5	2.3	1.2	–
e isolation & impact param.	1.5	1.1	0.4	–
e energy scale	0.5	0.3	0.3	–
e energy resolution	0.1	0.1	< 0.1	–
E_T^{miss} cluster energy scale	0.4	0.2	0.6	0.2
E_T^{miss} jet energy scale	0.1	0.1	0.1	0.1
E_T^{miss} jet energy resolution	0.3	0.3	0.4	0.2
E_T^{miss} pile-up	0.3	0.1	0.3	0.1
Muon trigger	–	0.1	0.1	0.3
Electron trigger	< 0.1	< 0.1	< 0.1	–
Event generator	0.4	0.4	0.4	0.4
PDF	1.2	1.2	1.2	1.2
QCD scale	0.4	0.4	0.4	0.4
Luminosity	1.8	1.8	1.8	1.8

ences observed between data and simulated samples are accounted for, and the uncertainties in the correction factors are used to evaluate the systematic uncertainties.

The uncertainties related to E_T^{miss} come mainly from the calibration of cluster and jet energies. The effects of event pile-up are evaluated from the distribution of total transverse energy as a function of $\langle \mu \rangle$.

Single-muon and single-electron trigger efficiencies are studied in samples of $Z \rightarrow \ell\ell$ events. Their effects on the $W^\pm Z$ measurement are small because the presence of three leptons provides redundancy for triggering.

The uncertainty in acceptance due to theoretical modelling in the event generator is estimated by comparing MC@NLO with another NLO generator, POWHEG BOX [29]. Uncertainties due to the PDFs are computed using the CT10 eigenvectors and the difference between the CT10 and MSTW 2008 [30] PDF sets. Uncertainties related to the factorization scale μ_F and renormalization scale μ_R are estimated by setting $\mu_F = \mu_R$ and varying this value up and down by a factor of two.

5 Background estimation

The major sources of background are summarized in Table 3. Data-driven methods are used to estimate the background from $Z + \text{jets}$ and $t\bar{t}$ production. Simulation is used for the remaining background sources, including ZZ , $t\bar{t} + W/Z$, and $Z + \gamma$ production. Background from other sources, such as heavy-flavour multi-jet events, is strongly suppressed by the requirement of three leptons with small d_0 , and is negligible. For studies of anomalous TGC (Sect. 6.2) and of normalized fiducial cross-sections (Sect. 6.3), the background is estimated separately in bins of the transverse momentum p_T^Z of the Z boson and the invariant mass m_{WZ} of the $W^\pm Z$ pair.

For background events with three true leptons from vector boson decays, the simulation models the acceptance and efficiency of the selection criteria reliably. The main background in this category is ZZ production, in which both Z bosons decay leptonically. The background distributions and

Table 3 Estimated numbers of background events. The errors include both statistical and systematic uncertainties

Source	eee	μee	$e\mu\mu$	$\mu\mu\mu$
$Z + \text{jets}$	8.8 ± 2.8	3.7 ± 2.3	10.2 ± 3.3	9.1 ± 5.5
ZZ	3.2 ± 0.2	4.9 ± 0.2	5.0 ± 0.1	7.9 ± 0.2
$Z + \gamma$	1.4 ± 0.7	–	2.3 ± 0.9	–
$t\bar{t}$	0.4 ± 0.4	1.7 ± 0.9	2.3 ± 1.1	2.4 ± 1.2
$t\bar{t} + W/Z$	0.7 ± 0.1	1.2 ± 0.1	1.3 ± 0.1	1.6 ± 0.1
Total	14.5 ± 2.9	11.5 ± 2.5	21.0 ± 3.5	21.0 ± 5.6

acceptances are determined directly from simulation for this process, and the theoretical cross-section is used for normalization. The total contribution of the ZZ background is 21.0 ± 0.7 events, where the error is dominated by the uncertainty on the theoretical cross-section.

Weak boson radiation associated with $t\bar{t}$ production can also produce three or more leptons and thus constitutes a significant background despite its small production cross-section. The total contribution of the $t\bar{t} + W/Z$ background is 4.7 ± 0.2 events. $Z + \gamma$ events can pass the selection criteria if the photon is misidentified as an electron. The contribution from this background is estimated from simulation to be 3.7 ± 1.1 events.

5.1 $Z + \text{jets}$ background

Production of a Z boson associated with jets is the largest source of background in this measurement. For a $Z + \text{jets}$ event to pass the event selection criteria, an isolated lepton must be reconstructed from one of the jets. The extra lepton is usually attributed to the W^\pm boson.

A *lepton-like jet* is defined as a jet that passes a few basic lepton selection criteria but not necessarily the full set of selection (for e) or isolation (for both e and μ) requirements. An event containing a Z boson and a lepton-like jet is a background event if the lepton-like jet passes all lepton selection criteria. Those that fail the lepton quality or isolation requirements constitute a control sample. To ensure that the control sample is as similar to the signal as possible, all other event selection criteria, including $E_T^{\text{miss}} > 25$ GeV, are applied.

In order to estimate the $Z + \text{jets}$ background from this control sample, the probability f of a lepton-like jet passing all lepton selection criteria is estimated in another control sample: events containing a Z boson and a lepton-like jet with $E_T^{\text{miss}} < 25$ GeV. This sample is dominated by $Z + \text{jets}$ events, and f can thus be directly measured. The contributions from other processes are subtracted using simulation. Simulation is also used to estimate the fraction of the $Z + \text{jets}$ background in which a lepton-like jet is attributed to the Z boson.

From the combination of the two control samples, the total $Z + \text{jets}$ background is estimated to be 31.9 ± 9.2 events. The largest source of uncertainty is the extrapolation from the $E_T^{\text{miss}} < 25$ GeV sample to the $E_T^{\text{miss}} > 25$ GeV sample, which was studied in simulation and in dijet data. Also included are the statistical uncertainties of the control samples and the uncertainties on the theoretical cross-sections of the processes subtracted from the control samples.

5.2 $t\bar{t}$ background

A large part of the top-quark background is eliminated by the impact-parameter and isolation requirements on the leptons, both of which reject lepton candidates originating in

jets. The rejection factors, however, cannot be reliably derived from simulation, and therefore data-driven corrections are applied to the simulated $t\bar{t}$ events to estimate them.

In this analysis, $t\bar{t}$ events are the only significant source of background that does not contain a Z boson. A control sample enriched in $t\bar{t}$ background events is defined by changing the charge combination of the dilepton pair from opposite sign to same sign. All other selection criteria are unchanged. Kinematic distributions of simulated $t\bar{t}$ events are similar in shape and normalization for same-charge and opposite-charge selections. The data-to-simulation ratio of the event yield in the same-sign sample is 2.2 ± 1.0 . This ratio is used to scale the $t\bar{t}$ background predicted in simulation. Using this procedure, the total contribution from the $t\bar{t}$ background is estimated to be 6.8 ± 3.2 events.

6 Results

The numbers of expected and observed events after applying all selection criteria are shown in Table 4. In total, 317 $W^\pm Z$ candidates are observed in data with 231 ± 8 signal (including final states with τ leptons) and 68 ± 10 background events expected. There are 206 $W^+ Z$ and 111 $W^- Z$ candidates, consistent with the expectations of 186 ± 11 and 110 ± 6 , respectively.

Figure 3 shows the distributions of the transverse momentum p_T^Z of the Z boson and the invariant mass m_{WZ} of the $W^\pm Z$ pair in selected events. To reconstruct m_{WZ} , the momenta of the three leptons are combined with E_T^{miss} , and a W^\pm boson mass constraint is used to solve for the z component p_z^v of the neutrino momentum. This generally leaves a two-fold ambiguity which is resolved by choosing the solution with the smaller $|p_z^v|$. In 27 % of the candidate events, the measured transverse mass is larger than the nominal W^\pm mass, and no real solutions exist for p_z^v . The most likely cause is that the measured E_T^{miss} is larger than the actual neutrino p_T . In this case, the best estimate is obtained by choosing the real part of the complex solutions, essentially reducing the magnitude of E_T^{miss} until a physical solution appears. The data distributions are compared with the expected SM signal and background. The shapes of the $Z + \text{jets}$ and $t\bar{t}$ distributions are taken from simulation and scaled according to the data-driven estimates.

Table 4 Summary of observed numbers of events N_{obs} and expected signal N_{sig} and background N_{bkg} contributions. N_{sig} includes the contribution from $W^\pm Z \rightarrow \tau X$

	eee	μee	$e\mu\mu$	$\mu\mu\mu$
N_{obs}	56	75	78	108
N_{sig}	38.9 ± 2.1	54.0 ± 2.2	56.6 ± 1.7	81.7 ± 2.1
N_{bkg}	14.5 ± 2.9	11.5 ± 2.5	21.0 ± 3.5	21.0 ± 5.6

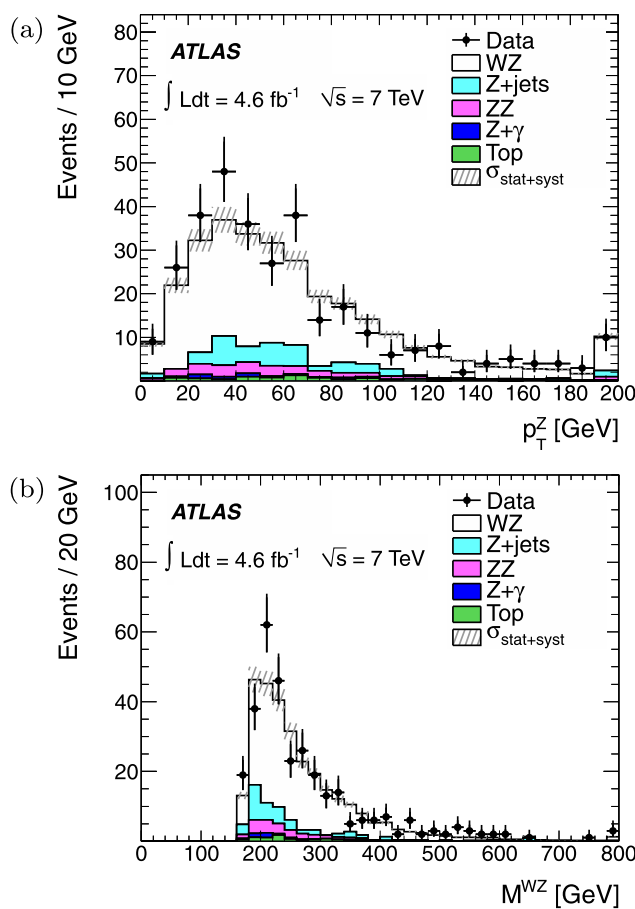


Fig. 3 Distributions of the $W^\pm Z$ candidates after all selection. **(a)** Transverse momentum p_T^Z of the Z boson. **(b)** Invariant mass m_{WZ} of the $W^\pm Z$ pair. The shaded bands indicate the total statistical and systematic uncertainties of the prediction. For $Z + \text{jets}$ and $t\bar{t}$, the expected shape is taken from simulation but the normalization is taken from the data-driven estimates. The rightmost bins include overflow

6.1 Cross-section measurement

Two cross-sections are extracted from the number of observed events. One is the fiducial $W^\pm Z \rightarrow \ell^\pm \nu \ell^+ \ell^-$ cross-section in a region of final-state phase space defined by the event selection criteria, the other is the total $W^\pm Z$ production cross-section. To extract the total cross-section, theoretical predictions must be used to extrapolate the measured event yield through the experimentally inaccessible part of the phase space, introducing additional theoretical uncertainties. The fiducial cross-section is free from such extrapolation, and is therefore less sensitive to theoretical uncertainties than the total cross-section.

In order to combine the different channels, a common phase space region is defined in which a fiducial cross-section is extracted. The common phase space is defined as $p_T^{\mu,e} > 15$ GeV for the leptons from the decay of the Z bosons, $p_T^{\mu,e} > 20$ GeV for the leptons from the decay of the W^\pm bosons, $|\eta^{\mu,e}| < 2.5$, $p_T^\nu > 25$ GeV, $|m_{\ell\ell} - m_Z| <$

10 GeV, and $M_T^W > 20$ GeV, to approximate the event selection. In simulated events, the momenta of photons that are within $\Delta R = 0.1$ of one of the three leptons are added to the lepton momentum. In addition, a separation of $\Delta R > 0.3$ between the two leptons of all possible pairings of the three leptons is required. This requirement emulates the isolation criteria applied to the leptons, which tend to reduce the signal acceptance for events with very large Z boson momenta. The definition of the fiducial phase space is identical to that used in Ref. [6] except for the requirement of $\Delta R > 0.3$ between the leptons.

For a given channel $W^\pm Z \rightarrow \ell^\pm \nu \ell^+ \ell^-$, where ℓ is either e or μ , the fiducial cross-section is calculated from

$$\sigma_{WZ}^{\text{fid}} = \frac{N_{\text{obs}} - N_{\text{bkg}}}{\int \mathcal{L} dt \cdot C_{WZ}} \left(1 - \frac{N_\tau^{\text{MC}}}{N_{\text{sig}}^{\text{MC}}} \right), \quad (2)$$

where N_{obs} and N_{bkg} denote the number of observed and background events respectively, $\int \mathcal{L} dt$ is the integrated luminosity, and C_{WZ} is the ratio of the number of accepted signal events to the number of generated events in the fiducial phase space. Corrections are applied to C_{WZ} to account for measured differences in trigger and reconstruction efficiencies between simulated and data samples and for the extrapolation to the fiducial phase space. The contribution from τ lepton decays, approximately 4 %, is removed from the fiducial cross-section definition by the term in parentheses, where N_τ^{MC} is the number of accepted simulated $W^\pm Z$ events in which at least one of the bosons decays into τ , and $N_{\text{sig}}^{\text{MC}}$ is the number of accepted simulated $W^\pm Z$ events with decays into any lepton. Since the fiducial phase space is defined by the kinematics of the final-state leptons, the calculated cross-section implicitly includes the leptonic branching fractions of the W^\pm and Z bosons.

The total cross-section is defined in the dilepton invariant mass range of $66 < m_{\ell\ell} < 116$ GeV for $Z \rightarrow \ell\ell$. It is computed as:

$$\sigma_{WZ}^{\text{tot}} = \frac{N_{\text{obs}} - N_{\text{bkg}}}{\int \mathcal{L} dt \cdot \mathcal{B}_W \mathcal{B}_Z A_{WZ} C_{WZ}} \left(1 - \frac{N_\tau^{\text{MC}}}{N_{\text{sig}}^{\text{MC}}} \right) \quad (3)$$

where \mathcal{B}_W and \mathcal{B}_Z are the W and Z leptonic branching fractions, respectively, and A_{WZ} is the ratio of the number of events within the fiducial phase space to the number of events within $66 < m_{\ell\ell} < 116$ GeV. The ratio A_{WZ} calculated using MC@NLO equals 0.330, 0.332, 0.333, and 0.338 for the eee , μee , $e\mu\mu$, and $\mu\mu\mu$ channels, respectively. The differences are due to the FSR photons emitted outside the $\Delta R = 0.1$ cone around the electrons.

Cross-section measurements are extracted using a maximum-likelihood method to combine the four channels. The likelihood function is defined as

$$L(\sigma, \mathbf{x}) = \prod_{i=1}^4 \text{Pois}(N_{\text{obs}}^i, N_s^i(\sigma, \mathbf{x}) + N_b^i(\mathbf{x})) \cdot e^{-\frac{\mathbf{x}}{2}} \quad (4)$$

where $\text{Pois}(N_{\text{obs}}^i, N_s^i + N_b^i)$ is the Poisson probability of observing N_{obs}^i events in channel i when N_s^i signal and N_b^i background events are expected. The nuisance parameters \mathbf{x} affect N_s^i and N_b^i as

$$N_s^i(\sigma, \mathbf{x}) = N_s^i(\sigma, 0) \left(1 + \sum_k x_k S_k^i \right), \quad (5)$$

$$N_b^i(\mathbf{x}) = N_b^i(0) \left(1 + \sum_k x_k B_k^i \right), \quad (6)$$

where S_k^i and B_k^i are the relative systematic uncertainties on the signal and background, respectively, due to the k -th source of systematic uncertainty.

To find the most probable value of σ (fiducial or total) the negative log-likelihood function (from Eq. (4)) is minimized simultaneously over σ and all the nuisance parameters x_k . The final results for the combined fiducial and total cross-sections are

$$\sigma_{WZ}^{\text{fid}} = 92^{+7}_{-6}(\text{stat.}) \pm 4(\text{syst.}) \pm 2(\text{lumi.}) \text{ fb},$$

$$\sigma_{WZ}^{\text{tot}} = 19.0^{+1.4}_{-1.3}(\text{stat.}) \pm 0.9(\text{syst.}) \pm 0.4(\text{lumi.}) \text{ pb}.$$

The fiducial cross-section σ_{WZ}^{fid} is the sum of the four channels. Cross-sections extracted separately for the four channels agree within their uncertainties. The uncertainties are estimated by taking the difference between the cross-section at the minimum of the negative log-likelihood function and the cross-section where the negative log-likelihood is 0.5 units above the minimum in the direction of the fit parameter σ . The likelihood is maximized over the nuisance parameters for each σ . The systematic uncertainties include all sources except luminosity. Correlations between the signal and background uncertainties owing to common sources of systematics are taken into account in the definition of the likelihood. Table 5 summarizes the systematic uncertainties on the cross-sections from different sources. The largest single source of systematic uncertainty is the data-driven estimate of the background contributions, dominated by that for $Z + \text{jets}$ production ($\pm 3.8\%$).

6.2 Anomalous triple gauge couplings

General expressions for the effective Lagrangian for the WWZ vertex can be found in Refs. [31, 32]. Retaining only terms that separately conserve charge conjugation C and parity P , the Lagrangian reduces to

$$\begin{aligned} \frac{\mathcal{L}_{WWZ}}{g_{WWZ}} = i & \left[g_1^Z (W_{\mu\nu}^\dagger W^\mu Z^\nu - W_{\mu\nu} W^{\dagger\mu} Z^\nu) \right. \\ & \left. + \kappa_Z W_\mu^\dagger W_\nu Z^{\mu\nu} + \frac{\lambda_Z}{m_W^2} W_{\rho\mu}^\dagger W_\nu^\mu Z^{\nu\rho} \right] \end{aligned} \quad (7)$$

Table 5 Systematic uncertainties, in %, on the fiducial and total cross-sections. The background uncertainties are split into data-driven estimates ($Z + \text{jets}$ and $t\bar{t}$) and estimates from simulation (all other processes)

Source	σ_{WZ}^{fid}	σ_{WZ}^{tot}
μ reconstruction	0.7	0.7
e reconstruction	2.1	2.0
E_T^{miss} reconstruction	0.5	0.5
Trigger	0.2	0.2
Signal MC statistics	0.5	0.5
Background data-driven	4.0	4.0
Background MC estimates	0.4	0.4
Event generator	–	0.4
PDF	–	1.2
QCD scale	–	0.4
Total	4.6	4.8
Luminosity	1.8	1.8

where $g_{WWZ} = -e \cot \theta_W$, e is the elementary charge, θ_W is the weak mixing angle, W_μ and Z_μ are the W and Z boson wave functions, $X_{\mu\nu} \equiv \partial_\mu X_\nu - \partial_\nu X_\mu$ for $X = W$ or Z , and g_1^Z , κ_Z , and λ_Z are dimensionless coupling constants. The SM predicts $g_1^Z = 1$, $\kappa_Z = 1$, and $\lambda_Z = 0$. This analysis sets limits on possible deviations of these parameters from their SM values, i.e. on $\Delta g_1^Z \equiv g_1^Z - 1$, $\Delta \kappa_Z \equiv \kappa_Z - 1$, and λ_Z , known as the anomalous TGC parameters. The $W^\pm Z$ production cross-section is a bilinear function of these anomalous TGCs.

To avoid tree-level unitarity violation, the anomalous couplings must vanish as \hat{s} , the four-momentum squared of the $W^\pm Z$ system, approaches infinity. To achieve this, an arbitrary form factor may be introduced [32]. Here the dipole form factor adopted is

$$\alpha(\hat{s}) = \frac{\alpha_0}{(1 + \hat{s}/\Lambda^2)^2} \quad (8)$$

where α stands for Δg_1^Z , $\Delta \kappa_Z$, or λ_Z , α_0 is the value of the anomalous coupling at low energy, and Λ is the cut-off scale, the scale at which new physics enters. The results are reported both with and without this form factor.

Since an enhancement in the cross-section due to an anomalous coupling would grow with \hat{s} , measurement sensitivity to anomalous TGCs is enhanced by binning the data in a kinematic variable related to \hat{s} . The transverse momentum p_T^Z of the Z boson provides a natural choice for such binning as it is strongly correlated with \hat{s} and can be directly reconstructed from the measured lepton momenta with good precision. The data are therefore divided into six bins in p_T^Z of width 30 GeV followed by a wide bin that includes 180–2000 GeV.

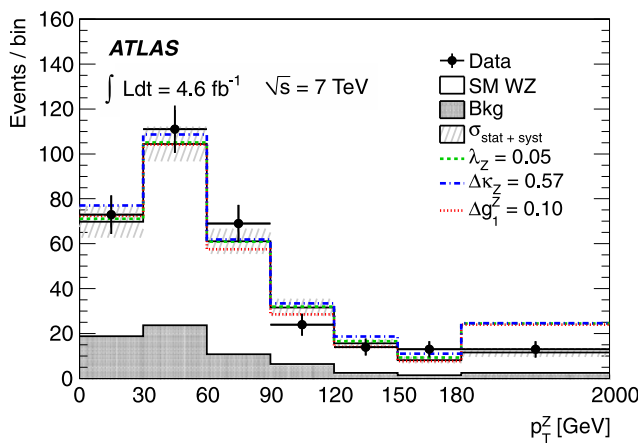


Fig. 4 Transverse momentum p_T^Z of the Z boson in $W^\pm Z$ candidate events. Data are shown together with expected background and signal events, assuming the Standard Model. Expected events in the case of anomalous TGC without form factor are also shown for illustration. The last bin is shortened for display purposes

MC@NLO [11] is used to generate $W^\pm Z$ events with non-SM TGC. The generator computes, for each event, a set of weights that can be used to reweight the full sample to any chosen set of anomalous couplings. This functionality is used to express the predicted signal yields in each bin of p_T^Z as a function of the anomalous couplings. Figure 4 shows the p_T^Z distribution of the selected events together with the SM prediction. Also shown for illustration are predictions with non-zero anomalous couplings without form factor: each coupling is increased to the expected 99 % confidence-level upper limit while keeping the other two couplings at the SM value. For this plot the 99 %, rather than 95 %, confidence-level upper limits are used to accentuate differences in shape. As expected, the largest deviations from the SM are in the last bin of p_T^Z , while the deviations in the lower- p_T^Z bins depend on which coupling is varied.

Frequentist confidence intervals are obtained on the anomalous couplings by forming a profile likelihood test incorporating the observed number of candidate events in each p_T^Z bin, the expected signal as a function of the anomalous couplings and the estimated number of background events [33]. The systematic uncertainties are included in the likelihood function as nuisance parameters with correlated Gaussian constraints. A point in the anomalous TGC space is accepted (rejected) at the 95 % confidence level if less (more) than 95 % of randomly generated pseudo-experiments exhibit a value of the profile likelihood ratio larger than that observed in data.

Table 6 summarizes the observed 95 % confidence intervals on the anomalous couplings Δg_1^Z , $\Delta \kappa_Z$, and λ_Z , with the cut-off scale $\Lambda = 2$ TeV and without the form factor. The limits on each anomalous TGC parameter are obtained with the other two anomalous TGC parameters set to zero. The expected intervals in Table 6 are medians of the 95 %

Table 6 Expected and observed 95 % confidence intervals on the anomalous couplings Δg_1^Z , $\Delta \kappa_Z$, and λ_Z . The expected intervals assume the Standard Model values for the couplings

	Observed $\Lambda = 2$ TeV	Observed no form factor	Expected no form factor
Δg_1^Z	[−0.074, 0.133]	[−0.057, 0.093]	[−0.046, 0.080]
$\Delta \kappa_Z$	[−0.42, 0.69]	[−0.37, 0.57]	[−0.33, 0.47]
λ_Z	[−0.064, 0.066]	[−0.046, 0.047]	[−0.041, 0.040]

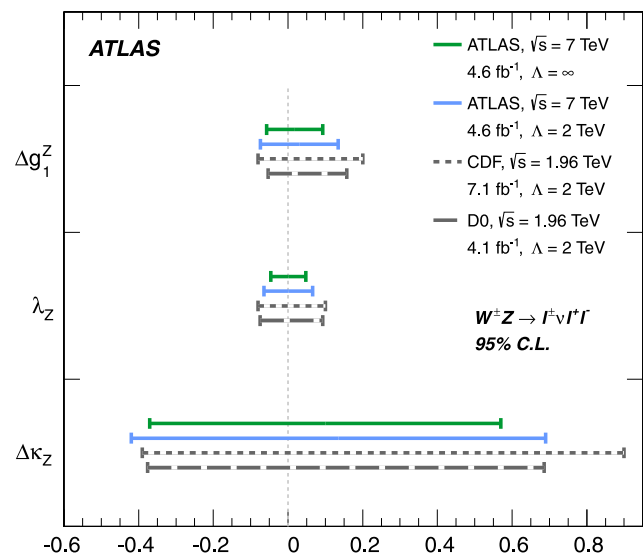


Fig. 5 95 % confidence intervals for anomalous TGCs from ATLAS (this work), CDF [34], and D0 [35]. Integrated luminosity, centre-of-mass energy and cut-off Λ for each experiment are shown

confidence-level upper and lower limits obtained in pseudo-experiments that assume the SM coupling. The widths of the expected and observed confidence intervals are dominated by statistical uncertainty. Figure 5 compares the observed limits with the Tevatron results [34, 35].

The 95 % confidence regions are shown as contours on the $(\Delta g_1^Z, \Delta \kappa_Z)$, $(\Delta g_1^Z, \lambda_Z)$, and $(\Delta \kappa_Z, \lambda_Z)$ planes in Fig. 6. In each plot the remaining parameter is set to the SM value. The limits were derived with no form factor.

6.3 Normalized fiducial cross-sections

The effective Lagrangian adopted in the TGC analysis in Sect. 6.2 allows us to probe non-SM physics with little model dependence. An alternative approach is to measure kinematic distributions, such as the p_T^Z spectrum, that could be compared with model-dependent theoretical predictions. For this purpose, it is necessary to convert the measured distributions to the underlying true distributions by unfolding the effects of the experimental acceptance and resolution. The iterative Bayesian unfolding proposed by D'Agostini [36] is applied here. An implementation of this

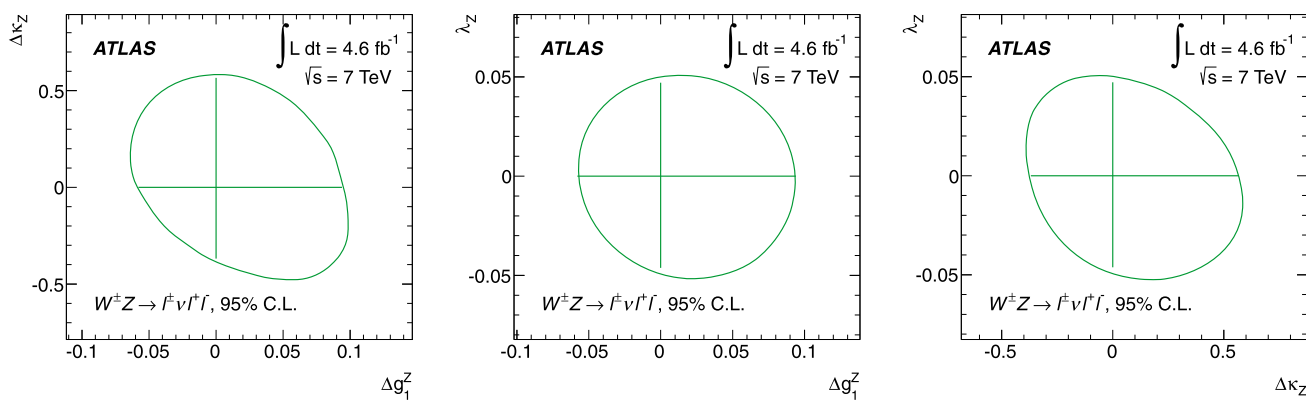


Fig. 6 Observed two-dimensional 95 % confidence regions on the anomalous couplings without form factor. The horizontal and vertical lines inside each contour correspond to the limits found in the one-dimensional fit procedure

technique has previously been used by ATLAS to unfold the p_T spectrum of inclusively produced W^\pm bosons [37].

In the unfolding of binned data, effects of the experimental acceptance and resolution are expressed in a response matrix, each element of which is the probability of an event in the i -th true bin being reconstructed in the j -th measured bin. In iterative Bayesian unfolding, the response matrix is combined with the measured spectrum to form a likelihood, which is then multiplied by a prior distribution to produce the posterior probability of the true spectrum. The SM prediction is used as the initial prior, and once the posterior probability is obtained, it is used as the prior for the next iteration after smoothing. The spectrum becomes insensitive to the initial prior after a few iterations. The number of iterations is adjusted to control the degree of regularization [36]. The differences between successive iterations can be used to estimate the stability of the unfolding method.

To achieve stable unfolding, that is, without excessive sensitivity to statistical fluctuations in data or to details of the unfolding technique, the measured quantity must be a good approximation to the underlying true quantity: the response matrix must be close to diagonal. The p_T^Z distribution used in the TGC analysis is a natural choice that has good resolution and sensitivity to possible new physics. The fractions of $W^\pm Z$ events that migrate between two p_T^Z bins are 2–7 %.

In addition to p_T^Z , the distribution of the diboson invariant mass m_{WZ} is also measured. The resolution of the reconstructed m_{WZ} is limited by the E_T^{miss} resolution. To avoid large bin-to-bin migration and achieve stable unfolding, three m_{WZ} bins are used: 170–270 GeV, 270–405 GeV, and 405–2500 GeV. With this binning, the fractions of events that migrate between two m_{WZ} bins are 13–17 %.

Figure 7 shows the fiducial cross-sections extracted in bins of p_T^Z and m_{WZ} , normalized by the sum of all bins. Comparison with the SM prediction shows good agreement.

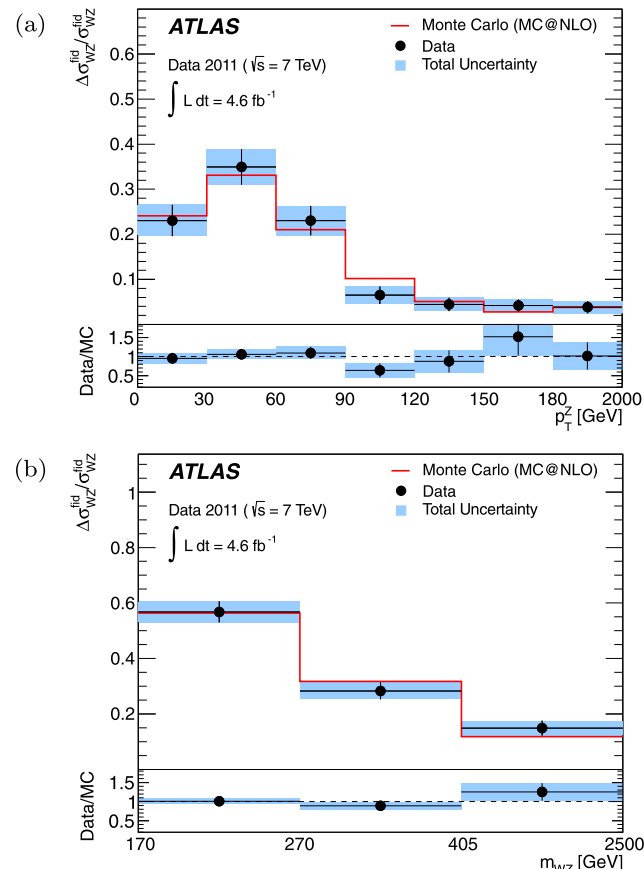


Fig. 7 Normalized fiducial cross-sections $\Delta\sigma_{WZ}^{\text{fid}}/\sigma_{WZ}^{\text{fid}}$ in bins of (a) p_T^Z and (b) m_{WZ} compared with the SM prediction. The total uncertainty contains statistical and systematic uncertainties added in quadrature

The corresponding numerical values are presented in Tables 7 and 8 for p_T^Z and m_{WZ} , respectively.

The dominant source of uncertainties on the normalized cross-sections is statistical. The statistical uncertainties are determined by a Monte Carlo method. Two thou-

Table 7 Normalized fiducial cross-sections and uncertainties in bins of p_T^Z

p_T^Z [GeV]	[0, 30]	[30, 60]	[60, 90]	[90, 120]	[120, 150]	[150, 180]	[180, 2000]
$\Delta\sigma_{WZ}^{\text{fid}}(p_T^Z)/\sigma_{WZ}^{\text{fid}}$	0.231	0.350	0.230	0.065	0.045	0.042	0.038
Uncertainty	0.034	0.039	0.033	0.019	0.015	0.014	0.013

Table 8 Normalized fiducial cross-sections and uncertainties in bins of m_{WZ}

m_{WZ} [GeV]	[170, 270]	[270, 405]	[405, 2500]
$\Delta\sigma_{WZ}^{\text{fid}}(m_{WZ})/\sigma_{WZ}^{\text{fid}}$	0.568	0.283	0.149
Uncertainty	0.038	0.030	0.027

and pseudo-experimental spectra are generated by fluctuating the content of each bin according to a Poisson distribution. The unfolding procedure is applied to each pseudo-experiment, and the r.m.s. of the results is taken as the statistical uncertainty. The systematic uncertainties are evaluated by varying the response matrix for each source of the uncertainty, and combining the resulting changes in the unfolded spectrum. Because of the normalization, the results are affected only by the uncertainties that depend on p_T^Z or m_{WZ} . The stability of the unfolding procedure is tested in two ways: firstly by comparing the unfolded spectra after two and after three iterations, and secondly by checking that the true variable distribution is correctly reproduced from a simulated sample generated with non-zero anomalous couplings.

7 Conclusion

Measurements of $W^\pm Z$ production in proton-proton collisions at $\sqrt{s} = 7$ TeV have been presented using a data sample with an integrated luminosity of 4.6 fb^{-1} , collected with the ATLAS detector at the LHC. The candidate $W^\pm Z$ events were selected in the fully leptonic final states with electrons, muons, and large missing transverse momentum. In total, 317 candidates were observed with a background expectation of 68 ± 10 events. The fiducial and total cross-sections are determined to be

$$\sigma_{WZ}^{\text{fid}} = 92^{+7}_{-6}(\text{stat.}) \pm 4(\text{syst.}) \pm 2(\text{lumi.}) \text{ fb},$$

and

$$\sigma_{WZ}^{\text{tot}} = 19.0^{+1.4}_{-1.3}(\text{stat.}) \pm 0.9(\text{syst.}) \pm 0.4(\text{lumi.}) \text{ pb},$$

respectively, where the fiducial cross-section is defined by $p_T^{\mu,e} > 15 \text{ GeV}$ for the leptons from the decay of the Z bosons, $p_T^{\mu,e} > 20 \text{ GeV}$ for the leptons from the decay of the W^\pm bosons, $|\eta^{\mu,e}| < 2.5$, $p_T^v > 25 \text{ GeV}$, $|m_{\ell\ell} - m_Z| < 10 \text{ GeV}$, $M_T^W > 20 \text{ GeV}$, and $\Delta R > 0.3$ between the two

leptons of all possible pairings of the three leptons. These results are significantly more precise than the earlier ATLAS measurement [6] which this paper supersedes. The total cross-section is consistent with the SM expectation of $17.6^{+1.1}_{-1.0} \text{ pb}$. Limits on anomalous triple gauge couplings have been derived based on the observed p_T^Z distribution. The 95 % confidence intervals are

$$\Delta g_1^Z \in [-0.057, 0.093]$$

$$\Delta\kappa_Z \in [-0.37, 0.57]$$

$$\lambda_Z \in [-0.046, 0.047]$$

without a form factor. The limits are again more stringent than the earlier ATLAS measurement. Normalized fiducial cross-sections have also been presented in bins of p_T^Z and m_{WZ} , and are in good agreement with SM predictions.

Acknowledgements We thank CERN for the very successful operation of the LHC, as well as the support staff from our institutions without whom ATLAS could not be operated efficiently.

We acknowledge the support of ANPCyT, Argentina; YerPhI, Armenia; ARC, Australia; BMWF, Austria; ANAS, Azerbaijan; SSTC, Belarus; CNPq and FAPESP, Brazil; NSERC, NRC and CFI, Canada; CERN; CONICYT, Chile; CAS, MOST and NSFC, China; COLCIENCIAS, Colombia; MSMT CR, MPO CR and VSC CR, Czech Republic; DNR, DNSRC and Lundbeck Foundation, Denmark; EPLANET and ERC, European Union; IN2P3-CNRS, CEA-DSM/IRFU, France; GNAS, Georgia; BMBF, DFG, HGF, MPG and AvH Foundation, Germany; GSRT, Greece; ISF, MINERVA, GIF, DIP and Benoziyo Center, Israel; INFN, Italy; MEXT and JSPS, Japan; CNRST, Morocco; FOM and NWO, Netherlands; RCN, Norway; MNiSW, Poland; GRICES and FCT, Portugal; MERYS (MECTS), Romania; MES of Russia and ROSATOM, Russian Federation; JINR; MSTD, Serbia; MSSR, Slovakia; ARRS and MVZT, Slovenia; DST/NRF, South Africa; MICINN, Spain; SRC and Wallenberg Foundation, Sweden; SER, SNSF and Cantons of Bern and Geneva, Switzerland; NSC, Taiwan; TAEK, Turkey; STFC, the Royal Society and Leverhulme Trust, United Kingdom; DOE and NSF, United States of America.

The crucial computing support from all WLCG partners is acknowledged gratefully, in particular from CERN and the ATLAS Tier-1 facilities at TRIUMF (Canada), NDGF (Denmark, Norway, Sweden), CC-IN2P3 (France), KIT/GridKA (Germany), INFN-CNAF (Italy), NL-T1 (Netherlands), PIC (Spain), ASGC (Taiwan), RAL (UK) and BNL (USA) and in the Tier-2 facilities worldwide.

Open Access This article is distributed under the terms of the Creative Commons Attribution License which permits any use, distribution, and reproduction in any medium, provided the original author(s) and the source are credited.

References

1. The ALEPH, CDF, D0, DELPHI, L3, OPAL, SLD Collaborations, the LEP Electroweak Working Group, the Tevatron Electroweak Working Group and the SLD electroweak and heavy flavour groups, [arXiv:1012.2367 \[hep-ex\]](#) (2010)
2. L. Dixon, Z. Kunszt, A. Signer, Phys. Rev. D **60**, 114037 (1999)
3. K.L. Adamson, D. de Florian, A. Signer, Phys. Rev. D **65**, 094041 (2002)
4. J.M. Campbell, R.K. Ellis, C. Williams, J. High Energy Phys. **1107**, 018 (2011)
5. H.L. Lai et al., Phys. Rev. D **82**, 074024 (2010)
6. ATLAS Collaboration, Phys. Lett. B **709**, 341 (2012)
7. ATLAS Collaboration, J. Instrum. **3**, S08003 (2008)
8. ATLAS Collaboration, Eur. Phys. J. C **70**, 823 (2010)
9. S. Agostinelli et al., Nucl. Instrum. Methods Phys. Res. A **506**, 250 (2003)
10. S. Frixione, B.R. Webber, J. High Energy Phys. **0206**, 029 (2002)
11. S. Frixione, F. Stoeckli, P. Torrielli, B.R. Webber, C.D. White, [arXiv:1010.0819 \[hep-ph\]](#) (2010)
12. G. Corcella et al., J. High Energy Phys. **0101**, 010 (2001)
13. J.M. Butterworth, J.R. Forshaw, M.H. Seymour, Z. Phys. C **72**, 637 (1996)
14. M.L. Mangano, M. Moretti, F. Piccinini, R. Pittau, A. Polosa, J. High Energy Phys. **0307**, 001 (2003)
15. S.P. Baranov, M. Smižanská, Phys. Rev. D **62**, 014012 (2000)
16. T. Sjöstrand et al., Comput. Phys. Commun. **135**, 238 (2001)
17. J. Alwall et al., J. High Energy Phys. **0709**, 028 (2007)
18. J.M. Campbell, R.K. Ellis, Phys. Rev. D **60**, 113006 (1999)
19. C. Anastasiou, L.J. Dixon, K. Melnikov, F. Petriello, Phys. Rev. D **69**, 094008 (2004)
20. R. Hamberg, W. van Neerven, T. Matsuura, Nucl. Phys. B **359**, 343 (1991). Erratum: Nucl. Phys. B **644**, 403 (2002)
21. T. Binoth, M. Ciccolini, N. Kauer, M. Krämer, J. High Energy Phys. **0612**, 046 (2006)
22. J.M. Campbell, R.K. Ellis, [arXiv:1204.5678 \[hep-ph\]](#) (2012)
23. A. Lazopoulos, T. McElmurry, K. Melnikov, F. Petriello, Phys. Lett. B **666**, 62 (2008)
24. P. Golonka, Z. Was, Eur. Phys. J. C **45**, 97 (2006)
25. S. Jadach, Z. Was, R. Decker, J. Kuhn, Comput. Phys. Commun. **76**, 361 (1993)
26. ATLAS Collaboration, Eur. Phys. J. C **72**, 1909 (2012)
27. ATLAS Collaboration, Eur. Phys. J. C **72**, 1844 (2012)
28. M. Cacciari, G.P. Salam, G. Soyez, J. High Energy Phys. **0804**, 063 (2008)
29. T. Melia, P. Nason, R. Ronisch, G. Zanderighi, J. High Energy Phys. **1111**, 078 (2011)
30. A. Martin, W. Stirling, R. Thorne, G. Watt, Eur. Phys. J. C **63**, 189 (2009)
31. K. Hagiwara, R.D. Peccei, D. Zeppenfeld, Nucl. Phys. B **282**, 253 (1987)
32. J. Ellison, J. Wudka, Annu. Rev. Nucl. Part. Sci. **48**, 33 (1998)
33. G. Cowan, K. Cranmer, E. Gross, O. Vitells, Eur. Phys. J. C **71**, 1554 (2011)
34. T. Aaltonen et al., Phys. Rev. D **86**, 031104 (2012). [arXiv:1202.6629 \[hep-ex\]](#)
35. V.M. Abazov et al., Phys. Lett. B **695**, 67 (2011)
36. G. D'Agostini, [arXiv:1010.0632 \[physics.data-an\]](#) (2010)
37. ATLAS Collaboration, Phys. Rev. D **85**, 012005 (2012)

The ATLAS Collaboration

G. Aad⁴⁸, T. Abajyan²¹, B. Abbott¹¹¹, J. Abdallah¹², S. Abdel Khalek¹¹⁵, A.A. Abdelalim⁴⁹, O. Abdinov¹¹, R. Aben¹⁰⁵, B. Abi¹¹², M. Abolins⁸⁸, O.S. AbouZeid¹⁵⁸, H. Abramowicz¹⁵³, H. Abreu¹³⁶, E. Acerbi^{89a,89b}, B.S. Acharya^{164a,164b}, L. Adamczyk³⁸, D.L. Adams²⁵, T.N. Addy⁵⁶, J. Adelman¹⁷⁶, S. Adomeit⁹⁸, P. Adragna⁷⁵, T. Adye¹²⁹, S. Aefsky²³, J.A. Aguilar-Saavedra^{124b,a}, M. Agustoni¹⁷, M. Aharrouche⁸¹, S.P. Ahlen²², F. Ahles⁴⁸, A. Ahmad¹⁴⁸, M. Ahsan⁴¹, G. Aielli^{133a,133b}, T. Akdogan^{19a}, T.P.A. Åkesson⁷⁹, G. Akimoto¹⁵⁵, A.V. Akimov⁹⁴, M.S. Alam², M.A. Alam⁷⁶, J. Albert¹⁶⁹, S. Albrand⁵⁵, M. Aleksić³⁰, I.N. Aleksandrov⁶⁴, F. Alessandria^{89a}, C. Alexa^{26a}, G. Alexander¹⁵³, G. Alexandre⁴⁹, T. Alexopoulos¹⁰, M. Alhroob^{164a,164c}, M. Aliev¹⁶, G. Alimonti^{89a}, J. Alison¹²⁰, B.M.M. Allbrooke¹⁸, P.P. Allport⁷³, S.E. Allwood-Spiers⁵³, J. Almond⁸², A. Aloisio^{102a,102b}, R. Alon¹⁷², A. Alonso⁷⁹, F. Alonso⁷⁰, B. Alvarez Gonzalez⁸⁸, M.G. Alviggi^{102a,102b}, K. Amako⁶⁵, C. Amelung²³, V.V. Ammosov^{128,*}, S.P. Amor Dos Santos^{124a}, A. Amorim^{124a,b}, N. Amram¹⁵³, C. Anastopoulos³⁰, L.S. Ancu¹⁷, N. Andari¹¹⁵, T. Andeen³⁵, C.F. Anders^{58b}, G. Anders^{58a}, K.J. Anderson³¹, A. Andreazza^{89a,89b}, V. Andrei^{58a}, M.-L. Andrieux⁵⁵, X.S. Anduaga⁷⁰, P. Anger⁴⁴, A. Angerami³⁵, F. Anghinolfi³⁰, A. Anisenkov¹⁰⁷, N. Anjos^{124a}, A. Annovi⁴⁷, A. Antonaki⁹, M. Antonelli⁴⁷, A. Antonov⁹⁶, J. Antos^{144b}, F. Anulli^{132a}, M. Aoki¹⁰¹, S. Aoun⁸³, L. Aperio Bella⁵, R. Apolle^{118,c}, G. Arabidze⁸⁸, I. Aracena¹⁴³, Y. Arai⁶⁵, A.T.H. Arce⁴⁵, S. Arfaoui¹⁴⁸, J-F. Arguin¹⁵, E. Arik^{19a,*}, M. Arik^{19a}, A.J. Armbruster⁸⁷, O. Arnaez⁸¹, V. Arnal⁸⁰, C. Arnault¹¹⁵, A. Artamonov⁹⁵, G. Artoni^{132a,132b}, D. Arutinov²¹, S. Asai¹⁵⁵, R. Asfandiyarov¹⁷³, S. Ask²⁸, B. Åsman^{146a,146b}, L. Asquith⁶, K. Assamagan²⁵, A. Astbury¹⁶⁹, M. Atkinson¹⁶⁵, B. Aubert⁵, E. Auge¹¹⁵, K. Augsten¹²⁷, M. Auousseau^{145a}, G. Avolio¹⁶³, R. Avramidou¹⁰, D. Axen¹⁶⁸, G. Azuelos^{93,d}, Y. Azuma¹⁵⁵, M.A. Baak³⁰, G. Baccaglioni^{89a}, C. Bacci^{134a,134b}, A.M. Bach¹⁵, H. Bachacou¹³⁶, K. Bachas³⁰, M. Backes⁴⁹, M. Backhaus²¹, E. Badescu^{26a}, P. Bagnai^{132a,132b}, S. Bahinipati³, Y. Bai^{33a}, D.C. Bailey¹⁵⁸, T. Bain¹⁵⁸, J.T. Baines¹²⁹, O.K. Baker¹⁷⁶, M.D. Baker²⁵, S. Baker⁷⁷, E. Banas³⁹, P. Banerjee⁹³, Sw. Banerjee¹⁷³, D. Banfi³⁰, A. Bangert¹⁵⁰, V. Bansal¹⁶⁹, H.S. Bansil¹⁸, L. Barak¹⁷², S.P. Baranov⁹⁴, A. Barbaro Galtieri¹⁵, T. Barber⁴⁸, E.L. Barberio⁸⁶, D. Barberis^{50a,50b}, M. Barbero²¹, D.Y. Bardin⁶⁴, T. Barillari⁹⁹, M. Barisonzi¹⁷⁵,

- T. Barklow¹⁴³, N. Barlow²⁸, B.M. Barnett¹²⁹, R.M. Barnett¹⁵, A. Baroncelli^{134a}, G. Barone⁴⁹, A.J. Barr¹¹⁸, F. Barreiro⁸⁰, J. Barreiro Guimaraes da Costa⁵⁷, P. Barrillon¹¹⁵, R. Bartoldus¹⁴³, A.E. Barton⁷¹, V. Bartsch¹⁴⁹, A. Basye¹⁶⁵, R.L. Bates⁵³, L. Batkova^{144a}, J.R. Batley²⁸, A. Battaglia¹⁷, M. Battistin³⁰, F. Bauer¹³⁶, H.S. Bawa^{143,e}, S. Beale⁹⁸, T. Beau⁷⁸, P.H. Beauchemin¹⁶¹, R. Beccerle^{50a}, P. Bechtle²¹, H.P. Beck¹⁷, A.K. Becker¹⁷⁵, S. Becker⁹⁸, M. Beckingham¹³⁸, K.H. Becks¹⁷⁵, A.J. Beddall^{19c}, A. Beddall^{19c}, S. Bedikian¹⁷⁶, V.A. Bednyakov⁶⁴, C.P. Bee⁸³, L.J. Beemster¹⁰⁵, M. Begel²⁵, S. Behar Harpaz¹⁵², P.K. Behera⁶², M. Beimforde⁹⁹, C. Belanger-Champagne⁸⁵, P.J. Bell⁴⁹, W.H. Bell⁴⁹, G. Bella¹⁵³, L. Bellagamba^{20a}, F. Bellina³⁰, M. Bellomo³⁰, A. Belloni⁵⁷, O. Beloborodova^{107,f}, K. Belotskiy⁹⁶, O. Beltramello³⁰, O. Benary¹⁵³, D. Benchekroun^{135a}, K. Bendtz^{146a,146b}, N. Benekos¹⁶⁵, Y. Benhammou¹⁵³, E. Benhar Noccioli⁴⁹, J.A. Benitez Garcia^{159b}, D.P. Benjamin⁴⁵, M. Benoit¹¹⁵, J.R. Bensinger²³, K. Benslama¹³⁰, S. Bentvelsen¹⁰⁵, D. Berge³⁰, E. Bergeaas Kuutmann⁴², N. Berger⁵, F. Berghaus¹⁶⁹, E. Berglund¹⁰⁵, J. Beringer¹⁵, P. Bernat⁷⁷, R. Bernhard⁴⁸, C. Bernius²⁵, T. Berry⁷⁶, C. Bertella⁸³, A. Bertin^{20a,20b}, F. Bertolucci^{122a,122b}, M.I. Besana^{89a,89b}, G.J. Besjes¹⁰⁴, N. Besson¹³⁶, S. Bethke⁹⁹, W. Bhimji⁴⁶, R.M. Bianchi³⁰, M. Bianco^{72a,72b}, O. Biebel⁹⁸, S.P. Bieniek⁷⁷, K. Bierwagen⁵⁴, J. Biesiada¹⁵, M. Biglietti^{134a}, H. Bilokon⁴⁷, M. Bindj^{20a,20b}, S. Binet¹¹⁵, A. Bingul^{19c}, C. Bini^{132a,132b}, C. Biscarat¹⁷⁸, B. Bittner⁹⁹, K.M. Black²², R.E. Blair⁶, J.-B. Blanchard¹³⁶, G. Blanchot³⁰, T. Blazek^{144a}, C. Blocker²³, J. Blocki³⁹, A. Blondel⁴⁹, W. Blum⁸¹, U. Blumenschein⁵⁴, G.J. Bobbink¹⁰⁵, V.B. Bobrovnikov¹⁰⁷, S.S. Bocchetta⁷⁹, A. Bocci⁴⁵, C.R. Boddy¹¹⁸, M. Boehler⁴⁸, J. Boek¹⁷⁵, N. Boelaert³⁶, J.A. Bogaerts³⁰, A. Bogdanchikov¹⁰⁷, A. Bogouch^{90,*}, C. Bohm^{146a}, J. Bohm¹²⁵, V. Boisvert⁷⁶, T. Bold³⁸, V. Boldea^{26a}, N.M. Bolnet¹³⁶, M. Bomben⁷⁸, M. Bona⁷⁵, M. Boonekamp¹³⁶, C.N. Booth¹³⁹, S. Bordoni⁷⁸, C. Borer¹⁷, A. Borisov¹²⁸, G. Borissov⁷¹, I. Borjanovic^{13a}, M. Borri⁸², S. Borroni⁸⁷, V. Bortolotto^{134a,134b}, K. Bos¹⁰⁵, D. Boscherini^{20a}, M. Bosman¹², H. Boterenbrood¹⁰⁵, J. Bouchami⁹³, J. Boudreau¹²³, E.V. Bouhova-Thacker⁷¹, D. Boumediene³⁴, C. Bourdarios¹¹⁵, N. Bousson⁸³, A. Boveia³¹, J. Boyd³⁰, I.R. Boyko⁶⁴, I. Bozovic-Jelisavcic^{13b}, J. Bracinik¹⁸, P. Branchini^{134a}, G.W. Brandenburg⁵⁷, A. Brandt⁸, G. Brandt¹¹⁸, O. Brandt⁵⁴, U. Bratzler¹⁵⁶, B. Brau⁸⁴, J.E. Brau¹¹⁴, H.M. Braun^{175,*}, S.F. Brazzale^{164a,164c}, B. Brelier¹⁵⁸, J. Bremer³⁰, K. Brendlinger¹²⁰, R. Brenner¹⁶⁶, S. Bressler¹⁷², D. Britton⁵³, F.M. Brochu²⁸, I. Brock²¹, R. Brock⁸⁸, F. Broggi^{89a}, C. Bromberg⁸⁸, J. Bronner⁹⁹, G. Brooijmans³⁵, T. Brooks⁷⁶, W.K. Brooks^{32b}, G. Brown⁸², H. Brown⁸, P.A. Bruckman de Renstrom³⁹, D. Bruncko^{144b}, R. Bruneliere⁴⁸, S. Brunet⁶⁰, A. Bruni^{20a}, G. Bruni^{20a}, M. Bruschi^{20a}, T. Buanes¹⁴, Q. Buat⁵⁵, F. Bucci⁴⁹, J. Buchanan¹¹⁸, P. Buchholz¹⁴¹, R.M. Buckingham¹¹⁸, A.G. Buckley⁴⁶, S.I. Buda^{26a}, I.A. Budagov⁶⁴, B. Budick¹⁰⁸, V. Büscher⁸¹, L. Bugge¹¹⁷, O. Bulekov⁹⁶, A.C. Bundock⁷³, M. Bunse⁴³, T. Buran¹¹⁷, H. Burckhart³⁰, S. Burdin⁷³, T. Burgess¹⁴, S. Burke¹²⁹, E. Busato³⁴, P. Bussey⁵³, C.P. Buszello¹⁶⁶, B. Butler¹⁴³, J.M. Butler²², C.M. Buttar⁵³, J.M. Butterworth⁷⁷, W. Buttlinger²⁸, S. Cabrera Urbán¹⁶⁷, D. Caforio^{20a,20b}, O. Cakir^{4a}, P. Calafuria¹⁵, G. Calderini⁷⁸, P. Calfayan⁹⁸, R. Calkins¹⁰⁶, L.P. Caloba^{24a}, R. Caloi^{132a,132b}, D. Calvet³⁴, S. Calvet³⁴, R. Camacho Toro³⁴, P. Camarri^{133a,133b}, D. Cameron¹¹⁷, L.M. Caminada¹⁵, R. Caminal Armadans¹², S. Campana³⁰, M. Campanelli⁷⁷, V. Canale^{102a,102b}, F. Canelli^{31,g}, A. Canepa^{159a}, J. Cantero⁸⁰, R. Cantrill⁷⁶, L. Capasso^{102a,102b}, M.D.M. Cappeans Garrido³⁰, I. Caprini^{26a}, M. Caprini^{26a}, D. Capriotti⁹⁹, M. Capua^{37a,37b}, R. Caputo⁸¹, R. Cardarelli^{133a}, T. Carli³⁰, G. Carlino^{102a}, L. Carminati^{89a,89b}, B. Caron⁸⁵, S. Caron¹⁰⁴, E. Carquin^{32b}, G.D. Carrillo Montoya¹⁷³, A.A. Carter⁷⁵, J.R. Carter²⁸, J. Carvalho^{124a,h}, D. Casadei¹⁰⁸, M.P. Casado¹², M. Cascella^{122a,122b}, C. Caso^{50a,50b,*}, A.M. Castaneda Hernandez^{173,i}, E. Castaneda-Miranda¹⁷³, V. Castillo Gimenez¹⁶⁷, N.F. Castro^{124a}, G. Cataldi^{72a}, P. Catastini⁵⁷, A. Catinaccio³⁰, J.R. Catmore³⁰, A. Cattai³⁰, G. Cattani^{133a,133b}, S. Caughran⁸⁸, V. Cavalieri¹⁶⁵, P. Cavalleri⁷⁸, D. Cavalli^{89a}, M. Cavalli-Sforza¹², V. Cavasinni^{122a,122b}, F. Ceradini^{134a,134b}, A.S. Cerqueira^{24b}, A. Cerri³⁰, L. Cerrito⁷⁵, F. Cerutti⁴⁷, S.A. Cetin^{19b}, A. Chafaq^{135a}, D. Chakraborty¹⁰⁶, I. Chalupkova¹²⁶, K. Chan³, P. Chang¹⁶⁵, B. Chapleau⁸⁵, J.D. Chapman²⁸, J.W. Chapman⁸⁷, E. Chareyre⁷⁸, D.G. Charlton¹⁸, V. Chavda⁸², C.A. Chavez Barajas³⁰, S. Cheatham⁸⁵, S. Chekanov⁶, S.V. Chekulaev^{159a}, G.A. Chelkov⁶⁴, M.A. Chelstowska¹⁰⁴, C. Chen⁶³, H. Chen²⁵, S. Chen^{33c}, X. Chen¹⁷³, Y. Chen³⁵, A. Cheplakov⁶⁴, R. Cherkaoui El Moursli^{135e}, V. Chernyatin²⁵, E. Cheu⁷, S.L. Cheung¹⁵⁸, L. Chevalier¹³⁶, G. Chieffari^{102a,102b}, L. Chikovani^{51a,*}, J.T. Childers³⁰, A. Chilingarov⁷¹, G. Chiodini^{72a}, A.S. Chisholm¹⁸, R.T. Chislett⁷⁷, A. Chitan^{26a}, M.V. Chizhov⁶⁴, G. Choudalakis³¹, S. Chouridou¹³⁷, I.A. Christidi⁷⁷, A. Christov⁴⁸, D. Chromek-Burckhart³⁰, M.L. Chu¹⁵¹, J. Chudoba¹²⁵, G. Ciappetti^{132a,132b}, A.K. Ciftci^{4a}, R. Ciftci^{4a}, D. Cinca³⁴, V. Cindro⁷⁴, C. Ciocca^{20a,20b}, A. Ciocio¹⁵, M. Cirilli⁸⁷, P. Cirkovic^{13b}, Z.H. Citron¹⁷², M. Citterio^{89a}, M. Ciubancan^{26a}, A. Clark⁴⁹, P.J. Clark⁴⁶, R.N. Clarke¹⁵, W. Cleland¹²³, J.C. Clemens⁸³, B. Clement⁵⁵, C. Clement^{146a,146b}, Y. Coadou⁸³, M. Cobal^{164a,164c}, A. Coccaro¹³⁸, J. Cochran⁶³, J.G. Cogan¹⁴³, J. Coggeshall¹⁶⁵, E. Cogneras¹⁷⁸, J. Colas⁵, S. Cole¹⁰⁶, A.P. Colijn¹⁰⁵, N.J. Collins¹⁸, C. Collins-Tooth⁵³, J. Collot⁵⁵, T. Colombo^{119a,119b}, G. Colon⁸⁴, P. Conde Muiño^{124a}, E. Coniavitis¹¹⁸, M.C. Conidi¹², S.M. Consonni^{89a,89b}, V. Consorti⁴⁸, S. Constantinescu^{26a}, C. Conta^{119a,119b}, G. Conti⁵⁷, F. Conventi^{102a,j}, M. Cooke¹⁵, B.D. Cooper⁷⁷, A.M. Cooper-Sarkar¹¹⁸, K. Copic¹⁵, T. Cornelissen¹⁷⁵, M. Corradi^{20a}, F. Corriveau^{85,k}, A. Cortes-Gonzalez¹⁶⁵, G. Cortiana⁹⁹, G. Costa^{89a}, M.J. Costa¹⁶⁷, D. Costanzo¹³⁹, D. Côté³⁰, L. Courneyea¹⁶⁹, G. Cowan⁷⁶, C. Cowden²⁸, B.E. Cox⁸², K. Cranmer¹⁰⁸, F. Crescioli^{122a,122b}, M. Cristinziani²¹, G. Crosetti^{37a,37b}, S. Crépé-Renaudin⁵⁵, C.-M. Cuciuc^{26a}, C. Cuenca Almenar¹⁷⁶, T. Cuhadar Donszelmann¹³⁹, M. Curatolo⁴⁷, C.J. Curtis¹⁸, C. Cuthbert¹⁵⁰, P. Cwetanski⁶⁰, H. Czirr¹⁴¹, P. Czodrowski⁴⁴,

- Z. Czyczula¹⁷⁶, S. D'Auria⁵³, M. D'Onofrio⁷³, A. D'Orazio^{132a,132b}, M.J. Da Cunha Sargedas De Sousa^{124a}, C. Da Via⁸², W. Dabrowski³⁸, A. Dafinca¹¹⁸, T. Dai⁸⁷, C. Dallapiccola⁸⁴, M. Dam³⁶, M. Dameri^{50a,50b}, D.S. Damiani¹³⁷, H.O. Danielsson³⁰, V. Dao⁴⁹, G. Darbo^{50a}, G.L. Darlea^{26b}, J.A. Dassoulas⁴², W. Davey²¹, T. Davidek¹²⁶, N. Davidson⁸⁶, R. Davidson⁷¹, E. Davies^{118,c}, M. Davies⁹³, O. Davignon⁷⁸, A.R. Davison⁷⁷, Y. Davygora^{58a}, E. Dawe¹⁴², I. Dawson¹³⁹, R.K. Daya-Ishmukhametova²³, K. De⁸, R. de Asmundis^{102a}, S. De Castro^{20a,20b}, S. De Cecco⁷⁸, J. de Graat⁹⁸, N. De Groot¹⁰⁴, P. de Jong¹⁰⁵, C. De La Taille¹¹⁵, H. De la Torre⁸⁰, F. De Lorenzi⁶³, L. de Mora⁷¹, L. De Nooij¹⁰⁵, D. De Pedis^{132a}, A. De Salvo^{132a}, U. De Sanctis^{164a,164c}, A. De Santo¹⁴⁹, J.B. De Vivie De Regie¹¹⁵, G. De Zorzi^{132a,132b}, W.J. Dearnaley⁷¹, R. Debbe²⁵, C. Debenedetti⁴⁶, B. Dechenaux⁵⁵, D.V. Dedovich⁶⁴, J. Degenhardt¹²⁰, C. Del Papa^{164a,164c}, J. Del Peso⁸⁰, T. Del Prete^{122a,122b}, T. Delemontex⁵⁵, M. Deliyergiyev⁷⁴, A. Dell'Acqua³⁰, L. Dell'Asta²², M. Della Pietra^{102a,j}, D. della Volpe^{102a,102b}, M. Delmastro⁵, P.A. Delsart⁵⁵, C. Deluca¹⁰⁵, S. Demers¹⁷⁶, M. Demichev⁶⁴, B. Demirkoz^{12,l}, J. Deng¹⁶³, S.P. Denisov¹²⁸, D. Derendarz³⁹, J.E. Derkaoui^{135d}, F. Derue⁷⁸, P. Dervan⁷³, K. Desch²¹, E. Devetak¹⁴⁸, P.O. Deviveiros¹⁰⁵, A. Dewhurst¹²⁹, B. DeWilde¹⁴⁸, S. Dhaliwal¹⁵⁸, R. Dhullipudi^{25,m}, A. Di Ciaccio^{133a,133b}, L. Di Ciaccio⁵, A. Di Girolamo³⁰, B. Di Girolamo³⁰, S. Di Luise^{134a,134b}, A. Di Mattia¹⁷³, B. Di Micco³⁰, R. Di Nardo⁴⁷, A. Di Simone^{133a,133b}, R. Di Sipio^{20a,20b}, M.A. Diaz^{32a}, E.B. Diehl⁸⁷, J. Dietrich⁴², T.A. Dietzsch^{58a}, S. Diglio⁸⁶, K. Dindar Yagci⁴⁰, J. Dingfelder²¹, F. Dinut^{26a}, C. Dionisi^{132a,132b}, P. Dita^{26a}, S. Dita^{26a}, F. Dittus³⁰, F. Djama⁸³, T. Djobava^{51b}, M.A.B. do Vale^{24c}, A. Do Valle Wemans^{124a,n}, T.K.O. Doan⁵, M. Dobbs⁸⁵, R. Dobinson^{30,*}, D. Dobos³⁰, E. Dobson^{30,o}, J. Dodd³⁵, C. Doglioni⁴⁹, T. Doherty⁵³, Y. Doi^{65,*}, J. Dolejsi¹²⁶, I. Dolenc⁷⁴, Z. Dolezal¹²⁶, B.A. Dolgoshein^{96,*}, T. Dohmae¹⁵⁵, M. Donadelli^{24d}, J. Donini³⁴, J. Dopke³⁰, A. Doria^{102a}, A. Dos Anjos¹⁷³, A. Dotti^{122a,122b}, M.T. Dova⁷⁰, A.D. Doxiadis¹⁰⁵, A.T. Doyle⁵³, N. Dressnandt¹²⁰, M. Dris¹⁰, J. Dubbert⁹⁹, S. Dube¹⁵, E. Duchovni¹⁷², G. Duckeck⁹⁸, D. Duda¹⁷⁵, A. Dudarev³⁰, F. Dudziak⁶³, M. Dührssen³⁰, I.P. Duerdorff⁸², L. Duflot¹¹⁵, M-A. Dufour⁸⁵, L. Duguid⁷⁶, M. Dunford³⁰, H. Duran Yildiz^{4a}, R. Duxfield¹³⁹, M. Dwuznik³⁸, F. Dydak³⁰, M. Düren⁵², W.L. Ebenstein⁴⁵, J. Ebke⁹⁸, S. Eckweiler⁸¹, K. Edmonds⁸¹, W. Edson², C.A. Edwards⁷⁶, N.C. Edwards⁵³, W. Ehrenfeld⁴², T. Eifert¹⁴³, G. Eigen¹⁴, K. Einsweiler¹⁵, E. Eisenhandler⁷⁵, T. Ekelof¹⁶⁶, M. El Kacimi^{135c}, M. Ellert¹⁶⁶, S. Elles⁵, F. Ellinghaus⁸¹, K. Ellis⁷⁵, N. Ellis³⁰, J. Elmsheuser⁹⁸, M. Elsing³⁰, D. Emeliyanov¹²⁹, R. Engelmann¹⁴⁸, A. Engl⁹⁸, B. Epp⁶¹, J. Erdmann⁵⁴, A. Ereditato¹⁷, D. Eriksson^{146a}, J. Ernst², M. Ernst²⁵, J. Ernwein¹³⁶, D. Errede¹⁶⁵, S. Errede¹⁶⁵, E. Ertel⁸¹, M. Escalier¹¹⁵, H. Esch⁴³, C. Escobar¹²³, X. Espinal Curull¹², B. Esposito⁴⁷, F. Etienne⁸³, A.I. Etienvre¹³⁶, E. Etzion¹⁵³, D. Evangelakou⁵⁴, H. Evans⁶⁰, L. Fabbri^{20a,20b}, C. Fabre³⁰, R.M. Fakhruddinov¹²⁸, S. Falciano^{132a}, Y. Fang¹⁷³, M. Fanti^{89a,89b}, A. Farbin⁸, A. Farilla^{134a}, J. Farley¹⁴⁸, T. Farooque¹⁵⁸, S. Farrell¹⁶³, S.M. Farrington¹⁷⁰, P. Farthouat³⁰, F. Fassi¹⁶⁷, P. Fassnacht³⁰, D. Fassouliotis⁹, B. Fatholahzadeh¹⁵⁸, A. Favareto^{89a,89b}, L. Fayard¹¹⁵, S. Fazio^{37a,37b}, R. Febbraro³⁴, P. Federic^{144a}, O.L. Fedin¹²¹, W. Fedorko⁸⁸, M. Fehling-Kaschek⁴⁸, L. Feligioni⁸³, D. Fellmann⁶, C. Feng^{33d}, E.J. Feng⁶, A.B. Fenjuk¹²⁸, J. Ferencei^{144b}, W. Fernando⁶, S. Ferrag⁵³, J. Ferrando⁵³, V. Ferrara⁴², A. Ferrari¹⁶⁶, P. Ferrari¹⁰⁵, R. Ferrari^{119a}, D.E. Ferreira de Lima⁵³, A. Ferrer¹⁶⁷, D. Ferrere⁴⁹, C. Ferretti⁸⁷, A. Ferretto Parodi^{50a,50b}, M. Fiascaris³¹, F. Fiedler⁸¹, A. Filipčič⁷⁴, F. Filthaut¹⁰⁴, M. Fincke-Keeler¹⁶⁹, M.C.N. Fiolhais^{124a,h}, L. Fiorini¹⁶⁷, A. Firan⁴⁰, G. Fischer⁴², M.J. Fisher¹⁰⁹, M. Flechi⁴⁸, I. Fleck¹⁴¹, J. Fleckner⁸¹, P. Fleischmann¹⁷⁴, S. Fleischmann¹⁷⁵, T. Flick¹⁷⁵, A. Floderus⁷⁹, L.R. Flores Castillo¹⁷³, M.J. Flowerdew⁹⁹, T. Fonseca Martin¹⁷, A. Formica¹³⁶, A. Forti⁸², D. Fortin^{159a}, D. Fournier¹¹⁵, A.J. Fowler⁴⁵, H. Fox⁷¹, P. Francavilla¹², M. Franchini^{20a,20b}, S. Franchino^{119a,119b}, D. Francis³⁰, T. Frank¹⁷², S. Franz³⁰, M. Fraternali^{119a,119b}, S. Fratina¹²⁰, S.T. French²⁸, C. Friedrich⁴², F. Friedrich⁴⁴, R. Froeschl³⁰, D. Froidevaux³⁰, J.A. Frost²⁸, C. Fukunaga¹⁵⁶, E. Fullana Torregrosa³⁰, B.G. Fulsom¹⁴³, J. Fuster¹⁶⁷, C. Gabaldon³⁰, O. Gabizon¹⁷², T. Gadfort²⁵, S. Gadomski⁴⁹, G. Gagliardi^{50a,50b}, P. Gagnon⁶⁰, C. Galea⁹⁸, B. Galhardo^{124a}, E.J. Gallas¹¹⁸, V. Gallo¹⁷, B.J. Gallop¹²⁹, P. Gallus¹²⁵, K.K. Gan¹⁰⁹, Y.S. Gao^{143,e}, A. Gaponenko¹⁵, F. Garberson¹⁷⁶, M. Garcia-Sciveres¹⁵, C. García¹⁶⁷, J.E. García Navarro¹⁶⁷, R.W. Gardner³¹, N. Garelli³⁰, H. Garitaonandia¹⁰⁵, V. Garonne³⁰, C. Gatti⁴⁷, G. Gaudio^{119a}, B. Gaur¹⁴¹, L. Gauthier¹³⁶, P. Gauzzi^{132a,132b}, I.L. Gavrilenco⁹⁴, C. Gay¹⁶⁸, G. Gaycken²¹, E.N. Gazis¹⁰, P. Ge^{33d}, Z. Gecse¹⁶⁸, C.N.P. Gee¹²⁹, D.A.A. Geerts¹⁰⁵, Ch. Geich-Gimbel²¹, K. Gellerstedt^{146a,146b}, C. Gemme^{50a}, A. Gemmell⁵³, M.H. Genest⁵⁵, S. Gentile^{132a,132b}, M. George⁵⁴, S. George⁷⁶, P. Gerlach¹⁷⁵, A. Gershon¹⁵³, C. Geweniger^{58a}, H. Ghazlane^{135b}, N. Ghodbane³⁴, B. Giacobbe^{20a}, S. Giagu^{132a,132b}, V. Giakoumopoulou⁹, V. Giangiobbe¹², F. Gianotti³⁰, B. Gibbard²⁵, A. Gibson¹⁵⁸, S.M. Gibson³⁰, D. Gillberg²⁹, A.R. Gillman¹²⁹, D.M. Gingrich^{3,d}, J. Ginzburg¹⁵³, N. Giokaris⁹, M.P. Giordani^{164c}, R. Giordano^{102a,102b}, F.M. Giorgi¹⁶, P. Giovannini⁹⁹, P.F. Giraud¹³⁶, D. Giugni^{89a}, M. Giunta⁹³, P. Giusti^{20a}, B.K. Gjelsten¹¹⁷, L.K. Gladilin⁹⁷, C. Glasman⁸⁰, J. Glatzer⁴⁸, A. Glazov⁴², K.W. Glitz¹⁷⁵, G.L. Glonti⁶⁴, J.R. Goddard⁷⁵, J. Godfrey¹⁴², J. Godlewski³⁰, M. Goebel⁴², T. Göpfert⁴⁴, C. Goeringer⁸¹, C. Gössling⁴³, S. Goldfarb⁸⁷, T. Golling¹⁷⁶, A. Gomes^{124a,b}, L.S. Gomez Fajardo⁴², R. Gonçalo⁷⁶, J. Goncalves Pinto Firmino Da Costa⁴², L. Gonella²¹, S. Gonzalez¹⁷³, S. González de la Hoz¹⁶⁷, G. Gonzalez Parra¹², M.L. Gonzalez Silva²⁷, S. Gonzalez-Sevilla⁴⁹, J.J. Goodson¹⁴⁸, L. Goossens³⁰, P.A. Gorbounov⁹⁵, H.A. Gordon²⁵, I. Gorelov¹⁰³, G. Gorfine¹⁷⁵, B. Gorini³⁰, E. Gorini^{72a,72b}, A. Gorišek⁷⁴, E. Gornicki³⁹, B. Gosdzik⁴², A.T. Goshaw⁶, M. Gosselink¹⁰⁵, M.I. Gostkin⁶⁴, I. Gough Eschrich¹⁶³, M. Gouighri^{135a},

- D. Goujdami^{135c}, M.P. Goulette⁴⁹, A.G. Goussiou¹³⁸, C. Goy⁵, S. Gozpinar²³, I. Grabowska-Bold³⁸, P. Grafström^{20a,20b}, K.-J. Grahn⁴², F. Grancagnolo^{72a}, S. Grancagnolo¹⁶, V. Grassi¹⁴⁸, V. Gratchev¹²¹, N. Grau³⁵, H.M. Gray³⁰, J.A. Gray¹⁴⁸, E. Graziani^{134a}, O.G. Grebenyuk¹²¹, T. Greenshaw⁷³, Z.D. Greenwood^{25,m}, K. Gregersen³⁶, I.M. Gregor⁴², P. Grenier¹⁴³, J. Griffiths⁸, N. Grigalashvili⁶⁴, A.A. Grillo¹³⁷, S. Grinstein¹², Ph. Gris³⁴, Y.V. Grishkevich⁹⁷, J.-F. Grivaz¹¹⁵, E. Gross¹⁷², J. Grosse-Knetter⁵⁴, J. Groth-Jensen¹⁷², K. Grybel¹⁴¹, D. Guest¹⁷⁶, C. Guicheney³⁴, S. Guindon⁵⁴, U. Gul⁵³, H. Guler^{85,p}, J. Gunther¹²⁵, B. Guo¹⁵⁸, J. Guo³⁵, P. Gutierrez¹¹¹, N. Guttman¹⁵³, O. Gutzwiller¹⁷³, C. Guyot¹³⁶, C. Gwenlan¹¹⁸, C.B. Gwilliam⁷³, A. Haas¹⁴³, S. Haas³⁰, C. Haber¹⁵, H.K. Hadavand⁴⁰, D.R. Hadley¹⁸, P. Haefner²¹, F. Hahn³⁰, S. Haider³⁰, Z. Hajduk³⁹, H. Hakobyan¹⁷⁷, D. Hall¹¹⁸, J. Haller⁵⁴, K. Hamacher¹⁷⁵, P. Hamal¹¹³, K. Hamano⁸⁶, M. Hamer⁵⁴, A. Hamilton^{145b,q}, S. Hamilton¹⁶¹, L. Han^{33b}, K. Hanagaki¹¹⁶, K. Hanawa¹⁶⁰, M. Hance¹⁵, C. Handel⁸¹, P. Hanke^{58a}, J.R. Hansen³⁶, J.B. Hansen³⁶, J.D. Hansen³⁶, P.H. Hansen¹⁴³, K. Hara¹⁶⁰, G.A. Hare¹³⁷, T. Harenberg¹⁷⁵, S. Harkusha⁹⁰, D. Harper⁸⁷, R.D. Harrington⁴⁶, O.M. Harris¹³⁸, J. Hartert⁴⁸, F. Hartjes¹⁰⁵, T. Haruyama⁶⁵, A. Harvey⁵⁶, S. Hasegawa¹⁰¹, Y. Hasegawa¹⁴⁰, S. Hassani¹³⁶, S. Haug¹⁷, M. Hauschild³⁰, R. Hauser⁸⁸, M. Havranek²¹, C.M. Hawkes¹⁸, R.J. Hawkings³⁰, A.D. Hawkins⁷⁹, D. Hawkins¹⁶³, T. Hayakawa⁶⁶, T. Hayashi¹⁶⁰, D. Hayden⁷⁶, C.P. Hays¹¹⁸, H.S. Hayward⁷³, S.J. Haywood¹²⁹, M. He^{33d}, S.J. Head¹⁸, V. Hedberg⁷⁹, L. Heelan⁸, S. Heim⁸⁸, B. Heinemann¹⁵, S. Heisterkamp³⁶, L. Helary²², C. Heller⁹⁸, M. Heller³⁰, S. Hellman^{146a,146b}, D. Hellmich²¹, C. Helsens¹², R.C.W. Henderson⁷¹, M. Henke^{58a}, A. Henrichs⁵⁴, A.M. Henriques Correia³⁰, S. Henrot-Versille¹¹⁵, C. Hensei⁵⁴, T. Henß¹⁷⁵, C.M. Hernandez⁸, Y. Hernández Jiménez¹⁶⁷, R. Herrberg¹⁶, G. Herten⁴⁸, R. Hertenberger⁹⁸, L. Hervas³⁰, G.G. Hesketh⁷⁷, N.P. Hessey¹⁰⁵, E. Higón-Rodriguez¹⁶⁷, J.C. Hill²⁸, K.H. Hiller⁴², S. Hillert²¹, S.J. Hillier¹⁸, I. Hinchliffe¹⁵, E. Hines¹²⁰, M. Hirose¹¹⁶, F. Hirsch⁴³, D. Hirschbuehl¹⁷⁵, J. Hobbs¹⁴⁸, N. Hod¹⁵³, M.C. Hodgkinson¹³⁹, P. Hodgson¹³⁹, A. Hoecker³⁰, M.R. Hoeferkamp¹⁰³, J. Hoffman⁴⁰, D. Hoffmann⁸³, M. Hohlfeld⁸¹, M. Holder¹⁴¹, S.O. Holmgren^{146a}, T. Holy¹²⁷, J.L. Holzbauer⁸⁸, T.M. Hong¹²⁰, L. Hooft van Huysduynen¹⁰⁸, S. Horner⁴⁸, J.-Y. Hostachy⁵⁵, S. Hou¹⁵¹, A. Houmada^{135a}, J. Howard¹¹⁸, J. Howarth⁸², I. Hristova¹⁶, J. Hrvnac¹¹⁵, T. Hrynn'ova⁵, P.J. Hsu⁸¹, S.-C. Hsu¹⁵, D. Hu³⁵, Z. Hubacek¹²⁷, F. Hubaut⁸³, F. Huegging²¹, A. Huettmann⁴², T.B. Huffman¹¹⁸, E.W. Hughes³⁵, G. Hughes⁷¹, M. Huhtinen³⁰, M. Hurwitz¹⁵, U. Husemann⁴², N. Huseynov^{64,r}, J. Huston⁸⁸, J. Huth⁵⁷, G. Iacobucci⁴⁹, G. Iakovidis¹⁰, M. Ibbotson⁸², I. Ibragimov¹⁴¹, L. Iconomidou-Fayard¹¹⁵, J. Idarraga¹¹⁵, P. Iengo^{102a}, O. Igonkina¹⁰⁵, Y. Ikegami⁶⁵, M. Ikeno⁶⁵, D. Iliadis¹⁵⁴, N. Ilic¹⁵⁸, T. Ince²¹, J. Inigo-Golfin³⁰, P. Ioannou⁹, M. Iodice^{134a}, K. Iordanidou⁹, V. Ippolito^{132a,132b}, A. Irles Quiles¹⁶⁷, C. Isaksson¹⁶⁶, M. Ishino⁶⁷, M. Ishitsuka¹⁵⁷, R. Ishmukhametov⁴⁰, C. Issever¹¹⁸, S. Istin^{19a}, A.V. Ivashin¹²⁸, W. Iwanski³⁹, H. Iwasaki⁶⁵, J.M. Izen⁴¹, V. Izzo^{102a}, B. Jackson¹²⁰, J.N. Jackson⁷³, P. Jackson¹, M.R. Jaekel³⁰, V. Jain⁶⁰, K. Jakobs⁴⁸, S. Jakobsen³⁶, T. Jakoubek¹²⁵, J. Jakubek¹²⁷, D.K. Jana¹¹¹, E. Jansen⁷⁷, H. Jansen³⁰, A. Jantsch⁹⁹, M. Janus⁴⁸, G. Jarlskog⁷⁹, L. Jeanty⁵⁷, I. Jen-La Plante³¹, D. Jennens⁸⁶, P. Jenni³⁰, A.E. Loevschall-Jensen³⁶, P. Jež³⁶, S. Jézéquel⁵, M.K. Jha^{20a}, H. Ji¹⁷³, W. Ji⁸¹, J. Jia¹⁴⁸, Y. Jiang^{33b}, M. Jimenez Belenguer⁴², S. Jin^{33a}, O. Jinnouchi¹⁵⁷, M.D. Joergensen³⁶, D. Joffe⁴⁰, M. Johansen^{146a,146b}, K.E. Johansson^{146a}, P. Johansson¹³⁹, S. Johnert⁴², K.A. Johns⁷, K. Jon-And^{146a,146b}, G. Jones¹⁷⁰, R.W.L. Jones⁷¹, T.J. Jones⁷³, C. Joram³⁰, P.M. Jorge^{124a}, K.D. Joshi⁸², J. Jovicevic¹⁴⁷, T. Jovin^{13b}, X. Ju¹⁷³, C.A. Jung⁴³, R.M. Jungst³⁰, V. Juraneck¹²⁵, P. Jussel⁶¹, A. Juste Rozas¹², S. Kabana¹⁷, M. Kaci¹⁶⁷, A. Kaczmarska³⁹, P. Kadlecik³⁶, M. Kado¹¹⁵, H. Kagan¹⁰⁹, M. Kagan⁵⁷, E. Kajomovitz¹⁵², S. Kalinin¹⁷⁵, L.V. Kalinovskaya⁶⁴, S. Kama⁴⁰, N. Kanaya¹⁵⁵, M. Kaneda³⁰, S. Kaneti²⁸, T. Kanno¹⁵⁷, V.A. Kantserov⁹⁶, J. Kanzaki⁶⁵, B. Kaplan¹⁰⁸, A. Kapliy³¹, J. Kaplon³⁰, D. Kar⁵³, M. Karagounis²¹, K. Karakostas¹⁰, M. Karnevskiy⁴², V. Kartvelishvili⁷¹, A.N. Karyukhin¹²⁸, L. Kashif¹⁷³, G. Kasieczka^{58b}, R.D. Kass¹⁰⁹, A. Kastanas¹⁴, M. Kataoka⁵, Y. Kataoka¹⁵⁵, E. Katsoufis¹⁰, J. Katzy⁴², V. Kaushik⁷, K. Kawagoe⁶⁹, T. Kawamoto¹⁵⁵, G. Kawamura⁸¹, M.S. Kay¹⁰⁵, S. Kazama¹⁵⁵, V.A. Kazanin¹⁰⁷, M.Y. Kazarinov⁶⁴, R. Keeler¹⁶⁹, P.T. Keener¹²⁰, R. Kehoe⁴⁰, M. Keij⁵⁴, G.D. Kekelidze⁶⁴, J.S. Keller¹³⁸, M. Kenyon⁵³, O. Kepka¹²⁵, N. Kerschen³⁰, B.P. Kerševan⁷⁴, S. Kersten¹⁷⁵, K. Kessoku¹⁵⁵, J. Keung¹⁵⁸, F. Khalil-zada¹¹, H. Khandanyan^{146a,146b}, A. Khanov¹¹², D. Kharchenko⁶⁴, A. Khodinov⁹⁶, A. Khomich^{58a}, T.J. Khoo²⁸, G. Khoriauli²¹, A. Khoroshilov¹⁷⁵, V. Khovanskii⁹⁵, E. Khramov⁶⁴, J. Khubua^{51b}, H. Kim^{146a,146b}, S.H. Kim¹⁶⁰, N. Kimura¹⁷¹, O. Kind¹⁶, B.T. King⁷³, M. King⁶⁶, R.S.B. King¹¹⁸, J. Kirk¹²⁹, A.E. Kiryunin⁹⁹, T. Kishimoto⁶⁶, D. Kisielewska³⁸, T. Kitamura⁶⁶, T. Kittelmann¹²³, K. Kiuchi¹⁶⁰, E. Kladiva^{144b}, M. Klein⁷³, U. Klein⁷³, K. Kleinknecht⁸¹, M. Klemetti⁸⁵, A. Klier¹⁷², P. Klimek^{146a,146b}, A. Klimentov²⁵, R. Klingenberg⁴³, J.A. Klinger⁸², E.B. Klinkby³⁶, T. Klioutchnikova³⁰, P.F. Klok¹⁰⁴, S. Klous¹⁰⁵, E.-E. Kluge^{58a}, T. Kluge⁷³, P. Kluit¹⁰⁵, S. Kluth⁹⁹, N.S. Knecht¹⁵⁸, E. Kneringer⁶¹, E.B.F.G. Knoops⁸³, A. Knue⁵⁴, B.R. Ko⁴⁵, T. Kobayashi¹⁵⁵, M. Kobel⁴⁴, M. Kocian¹⁴³, P. Kodys¹²⁶, K. Köneke³⁰, A.C. König¹⁰⁴, S. Koenig⁸¹, L. Köpke⁸¹, F. Koetsveld¹⁰⁴, P. Koevesarki²¹, T. Koffas²⁹, E. Koffeman¹⁰⁵, L.A. Kogan¹¹⁸, S. Kohlmann¹⁷⁵, F. Kohn⁵⁴, Z. Kohout¹²⁷, T. Kohriki⁶⁵, T. Koi¹⁴³, G.M. Kolachev^{107,*}, H. Kolanoski¹⁶, V. Kolesnikov⁶⁴, I. Koletsou^{89a}, J. Koll⁸⁸, M. Kollefrath⁴⁸, A.A. Komar⁹⁴, Y. Komori¹⁵⁵, T. Kondo⁶⁵, T. Kono^{42,s}, A.I. Kononov⁴⁸, R. Konoplich^{108,t}, N. Konstantinidis⁷⁷, S. Koperny³⁸, K. Korcyl³⁹, K. Kordas¹⁵⁴, A. Korn¹¹⁸, A. Korol¹⁰⁷, I. Korolkov¹², E.V. Korolkova¹³⁹, V.A. Korotkov¹²⁸, O. Kortner⁹⁹, S. Kortner⁹⁹, V.V. Kostyukhin²¹, S. Kotov⁹⁹, V.M. Kotov⁶⁴, A. Kotwal⁴⁵, C. Kourkoumelis⁹,

- V. Kouskoura¹⁵⁴, A. Koutsman^{159a}, R. Kowalewski¹⁶⁹, T.Z. Kowalski³⁸, W. Kozanecki¹³⁶, A.S. Kozhin¹²⁸, V. Kral¹²⁷, V.A. Kramarenko⁹⁷, G. Kramberger⁷⁴, M.W. Krasny⁷⁸, A. Krasznahorkay¹⁰⁸, J.K. Kraus²¹, S. Kreiss¹⁰⁸, F. Krejci¹²⁷, J. Kretzschmar⁷³, N. Krieger⁵⁴, P. Krieger¹⁵⁸, K. Kroeninger⁵⁴, H. Kroha⁹⁹, J. Kroll¹²⁰, J. Kroseberg²¹, J. Krstic^{13a}, U. Kruchonak⁶⁴, H. Krüger²¹, T. Krucker¹⁷, N. Krumnack⁶³, Z.V. Krumshteyn⁶⁴, T. Kubota⁸⁶, S. Kuday^{4a}, S. Kuehn⁴⁸, A. Kugel^{58c}, T. Kuhl⁴², D. Kuhn⁶¹, V. Kukhtin⁶⁴, Y. Kulchitsky⁹⁰, S. Kuleshov^{32b}, C. Kummer⁹⁸, M. Kuna⁷⁸, J. Kunckle¹²⁰, A. Kupco¹²⁵, H. Kurashige⁶⁶, M. Kurata¹⁶⁰, Y.A. Kurochkin⁹⁰, V. Kus¹²⁵, E.S. Kuwertz¹⁴⁷, M. Kuze¹⁵⁷, J. Kvita¹⁴², R. Kwee¹⁶, A. La Rosa⁴⁹, L. La Rotonda^{37a,37b}, L. Labarga⁸⁰, J. Labbe⁵, S. Lablak^{135a}, C. Lacasta¹⁶⁷, F. Lacava^{132a,132b}, H. Lacker¹⁶, D. Lacour⁷⁸, V.R. Lacuesta¹⁶⁷, E. Ladygin⁶⁴, R. Lafaye⁵, B. Laforge⁷⁸, T. Lagouri⁸⁰, S. Lai⁴⁸, E. Laisne⁵⁵, M. Lamanna³⁰, L. Lambourne⁷⁷, C.L. Lampen⁷, W. Lampl⁷, E. Lancon¹³⁶, U. Landgraf⁴⁸, M.P.J. Landon⁷⁵, J.L. Lane⁸², V.S. Lang^{58a}, C. Lange⁴², A.J. Lankford¹⁶³, F. Lanni²⁵, K. Lantzsch¹⁷⁵, S. Laplace⁷⁸, C. Lapoire²¹, J.F. Laporte¹³⁶, T. Lari^{89a}, A. Larner¹¹⁸, M. Lassnig³⁰, P. Laurelli⁴⁷, V. Lavorini^{37a,37b}, W. Lavrijzen¹⁵, P. Laycock⁷³, O. Le Dortz⁷⁸, E. Le Guirriec⁸³, C. Le Maner¹⁵⁸, E. Le Menedeu¹², T. LeCompte⁶, F. Ledroit-Guillon⁵⁵, H. Lee¹⁰⁵, J.S.H. Lee¹¹⁶, S.C. Lee¹⁵¹, L. Lee¹⁷⁶, M. Lefebvre¹⁶⁹, M. Legendre¹³⁶, F. Legger⁹⁸, C. Leggett¹⁵, M. Lehmacuer²¹, G. Lehmann Miotto³⁰, X. Lei⁷, M.A.L. Leite^{24d}, R. Leitner¹²⁶, D. Lellouch¹⁷², B. Lemmer⁵⁴, V. Lendermann^{58a}, K.J.C. Leney^{145b}, T. Lenz¹⁰⁵, G. Lenzen¹⁷⁵, B. Lenzi³⁰, K. Leonhardt⁴⁴, S. Leontsinis¹⁰, F. Lepold^{58a}, C. Leroy⁹³, J.-R. Lessard¹⁶⁹, C.G. Lester²⁸, C.M. Lester¹²⁰, J. Levêque⁵, D. Levin⁸⁷, L.J. Levinson¹⁷², A. Lewis¹¹⁸, G.H. Lewis¹⁰⁸, A.M. Leyko²¹, M. Leyton¹⁶, B. Li⁸³, H. Li^{173,u}, S. Li^{33b,v}, X. Li⁸⁷, Z. Liang^{118,w}, H. Liao³⁴, B. Liberti^{133a}, P. Lichard³⁰, M. Lichtnecker⁹⁸, K. Lie¹⁶⁵, W. Liebig¹⁴, C. Limbach²¹, A. Limosani⁸⁶, M. Limper⁶², S.C. Lin^{151,x}, F. Linde¹⁰⁵, J.T. Linnemann⁸⁸, E. Lipeles¹²⁰, A. Lipniacka¹⁴, T.M. Liss¹⁶⁵, D. Lissauer²⁵, A. Lister⁴⁹, A.M. Litke¹³⁷, C. Liu²⁹, D. Liu¹⁵¹, H. Liu⁸⁷, J.B. Liu⁸⁷, L. Liu⁸⁷, M. Liu^{33b}, Y. Liu^{33b}, M. Livan^{119a,119b}, S.S.A. Livermore¹¹⁸, A. Lleres⁵⁵, J. Llorente Merino⁸⁰, S.L. Lloyd⁷⁵, E. Lobodzinska⁴², P. Loch⁷, W.S. Lockman¹³⁷, T. Loddenkoetter²¹, F.K. Loebinger⁸², A. Loginov¹⁷⁶, C.W. Loh¹⁶⁸, T. Lohse¹⁶, K. Lohwasser⁴⁸, M. Lokajicek¹²⁵, V.P. Lombardo⁵, R.E. Long⁷¹, L. Lopes^{124a}, D. Lopez Mateos⁵⁷, J. Lorenz⁹⁸, N. Lorenzo Martinez¹¹⁵, M. Losada¹⁶², P. Loscutoff¹⁵, F. Lo Sterzo^{132a,132b}, M.J. Losty^{159a,*}, X. Lou⁴¹, A. Lounis¹¹⁵, K.F. Loureiro¹⁶², J. Love⁶, P.A. Love⁷¹, A.J. Lowe^{143,e}, F. Lu^{33a}, H.J. Lubatti¹³⁸, C. Luci^{132a,132b}, A. Lucotte⁵⁵, A. Ludwig⁴⁴, D. Ludwig⁴², I. Ludwig⁴⁸, J. Ludwig⁴⁸, F. Luehring⁶⁰, G. Luijckx¹⁰⁵, W. Lukas⁶¹, D. Lumb⁴⁸, L. Luminari^{132a}, E. Lund¹¹⁷, B. Lund-Jensen¹⁴⁷, B. Lundberg⁷⁹, J. Lundberg^{146a,146b}, O. Lundberg^{146a,146b}, J. Lundquist³⁶, M. Lungwitz⁸¹, D. Lynn²⁵, E. Lytken⁷⁹, H. Ma²⁵, L.L. Ma¹⁷³, G. Maccarrone⁴⁷, A. Macchiolo⁹⁹, B. Maček⁷⁴, J. Machado Miguens^{124a}, R. Mackeprang³⁶, R.J. Madaras¹⁵, H.J. Maddocks⁷¹, W.F. Mader⁴⁴, R. Maenner^{58c}, T. Maeno²⁵, P. Mättig¹⁷⁵, S. Mättig⁸¹, L. Magnoni¹⁶³, E. Magradze⁵⁴, K. Mahboubi⁴⁸, S. Mahmoud⁷³, G. Mahout¹⁸, C. Maiani¹³⁶, C. Maidantchik^{24a}, A. Mai^{124a,b}, S. Majewski²⁵, Y. Makida⁶⁵, N. Makovec¹¹⁵, P. Mal¹³⁶, B. Malaescu³⁰, Pa. Malecki³⁹, P. Malecki³⁹, V.P. Maleev¹²¹, F. Malek⁵⁵, U. Mallik⁶², D. Malon⁶, C. Malone¹⁴³, S. Maltezos¹⁰, V. Malyshev¹⁰⁷, S. Malyukov³⁰, R. Mamaghani⁹⁸, J. Mamuzic^{13b}, A. Manabe⁶⁵, L. Mandelli^{89a}, I. Mandic⁷⁴, R. Mandrysch¹⁶, J. Maneira^{124a}, A. Mandfredini⁹⁹, P.S. Mangeard⁸⁸, L. Manhaes de Andrade Filho^{24b}, J.A. Manjarres Ramos¹³⁶, A. Mann⁵⁴, P.M. Manning¹³⁷, A. Manousakis-Katsikakis⁹, B. Mansoulie¹³⁶, A. Mapelli³⁰, L. Mapelli³⁰, L. March⁸⁰, J.F. Marchand²⁹, F. Marchese^{133a,133b}, G. Marchiori⁷⁸, M. Marcisovsky¹²⁵, C.P. Marino¹⁶⁹, F. Marroquim^{24a}, Z. Marshall³⁰, F.K. Martens¹⁵⁸, L.F. Marti¹⁷, S. Marti-Garcia¹⁶⁷, B. Martin³⁰, B. Martin⁸⁸, J.P. Martin⁹³, T.A. Martin¹⁸, V.J. Martin⁴⁶, B. Martin dit Latour⁴⁹, S. Martin-Haugh¹⁴⁹, M. Martinez¹², V. Martinez Ootschoorn⁵⁷, A.C. Martyniuk¹⁶⁹, M. Marx⁸², F. Marzano^{132a}, A. Marzin¹¹¹, L. Masetti⁸¹, T. Mashimo¹⁵⁵, R. Mashinistov⁹⁴, J. Masik⁸², A.L. Maslennikov¹⁰⁷, I. Massa^{20a,20b}, G. Massaro¹⁰⁵, N. Massol⁵, P. Mastrandrea¹⁴⁸, A. Mastroberardino^{37a,37b}, T. Masubuchi¹⁵⁵, P. Matricon¹¹⁵, H. Matsunaga¹⁵⁵, T. Matsushita⁶⁶, C. Mattravers^{118,c}, J. Maurer⁸³, S.J. Maxfield⁷³, A. Mayne¹³⁹, R. Mazini¹⁵¹, M. Mazur²¹, L. Mazzaferro^{133a,133b}, M. Mazzanti^{89a}, J. Mc Donald⁸⁵, S.P. Mc Kee⁸⁷, A. McCarn¹⁶⁵, R.L. McCarthy¹⁴⁸, T.G. McCarthy²⁹, N.A. McCubbin¹²⁹, K.W. McFarlane^{56,*}, J.A. McFayden¹³⁹, G. Mchedlidze^{51b}, T. McLaughlan¹⁸, S.J. McMahon¹²⁹, R.A. McPherson^{169,k}, A. Meade⁸⁴, J. Mechlich¹⁰⁵, M. Mechtel¹⁷⁵, M. Medinnis⁴², R. Meera-Lebbai¹¹¹, T. Meguro¹¹⁶, R. Mehdiyev⁹³, S. Mehlhase³⁶, A. Mehta⁷³, K. Meier^{58a}, B. Meirose⁷⁹, C. Melachrinos³¹, B.R. Mellado Garcia¹⁷³, F. Meloni^{89a,89b}, L. Mendoza Navas¹⁶², Z. Meng^{151,u}, A. Mengarelli^{20a,20b}, S. Menke⁹⁹, E. Meoni¹⁶¹, K.M. Mercurio⁵⁷, P. Mermod⁴⁹, L. Merola^{102a,102b}, C. Meroni^{89a}, F.S. Merritt³¹, H. Merritt¹⁰⁹, A. Messina^{30,y}, J. Metcalfe²⁵, A.S. Mete¹⁶³, C. Meyer⁸¹, C. Meyer³¹, J.-P. Meyer¹³⁶, J. Meyer¹⁷⁴, J. Meyer⁵⁴, T.C. Meyer³⁰, J. Miao^{33d}, S. Michal³⁰, L. Micu^{26a}, R.P. Middleton¹²⁹, S. Migas⁷³, L. Mijović¹³⁶, G. Mikenberg¹⁷², M. Mikestikova¹²⁵, M. Mikuž⁷⁴, D.W. Miller³¹, R.J. Miller⁸⁸, W.J. Mills¹⁶⁸, C. Mills⁵⁷, A. Milov¹⁷², D.A. Milstead^{146a,146b}, D. Milstein¹⁷², A.A. Minaenko¹²⁸, M. Miñano Moya¹⁶⁷, I.A. Minashvili⁶⁴, A.I. Mincer¹⁰⁸, B. Mindur³⁸, M. Mineev⁶⁴, Y. Ming¹⁷³, L.M. Mir¹², G. Mirabelli^{132a}, J. Mitrevski¹³⁷, V.A. Mitsou¹⁶⁷, S. Mitsui⁶⁵, P.S. Miyagawa¹³⁹, J.U. Mjörnmark⁷⁹, T. Moa^{146a,146b}, V. Moeller²⁸, K. Möning⁴², N. Möser²¹, S. Mohapatra¹⁴⁸, W. Mohr⁴⁸, R. Moles-Valls¹⁶⁷, A. Molfetas³⁰, J. Monk⁷⁷, E. Monnier⁸³, J. Montejo Berlingen¹², F. Monticelli⁷⁰, S. Monzani^{20a,20b}, R.W. Moore³, G.F. Moorhead⁸⁶, C. Mora Herrera⁴⁹, A. Moraes⁵³, N. Morange¹³⁶, J. Morel⁵⁴, G. Morello^{37a,37b}, D. Moreno⁸¹, M. Moreno

- Llácer¹⁶⁷, P. Morettini^{50a}, M. Morgenstern⁴⁴, M. Morii⁵⁷, A.K. Morley³⁰, G. Mornacchi³⁰, J.D. Morris⁷⁵, L. Morvaj¹⁰¹, H.G. Moser⁹⁹, M. Mosidze^{51b}, J. Moss¹⁰⁹, R. Mount¹⁴³, E. Mountricha^{10,z}, S.V. Mouraviev^{94,*}, E.J.W. Moyse⁸⁴, F. Mueller^{58a}, J. Mueller¹²³, K. Mueller²¹, T.A. Müller⁹⁸, T. Mueller⁸¹, D. Muenstermann³⁰, Y. Munwes¹⁵³, W.J. Murray¹²⁹, I. Mussche¹⁰⁵, E. Musto^{102a,102b}, A.G. Myagkov¹²⁸, M. Myska¹²⁵, J. Nadal¹², K. Nagai¹⁶⁰, R. Nagai¹⁵⁷, K. Nagano⁶⁵, A. Nagarkar¹⁰⁹, Y. Nagasaka⁵⁹, M. Nagel⁹⁹, A.M. Nairz³⁰, Y. Nakahama³⁰, K. Nakamura¹⁵⁵, T. Nakamura¹⁵⁵, I. Nakano¹¹⁰, G. Nanava²¹, A. Napier¹⁶¹, R. Narayan^{58b}, M. Nash^{77,c}, T. Nattermann²¹, T. Naumann⁴², G. Navarro¹⁶², H.A. Neal⁸⁷, P.Yu. Nechaeva⁹⁴, T.J. Neep⁸², A. Negri^{119a,119b}, G. Negri³⁰, M. Negrini^{20a}, S. Nektarijevic⁴⁹, A. Nelson¹⁶³, T.K. Nelson¹⁴³, S. Nemecek¹²⁵, P. Nemethy¹⁰⁸, A.A. Nepomuceno^{24a}, M. Nessi^{30,aa}, M.S. Neubauer¹⁶⁵, M. Neumann¹⁷⁵, A. Neusiedl⁸¹, R.M. Neves¹⁰⁸, P. Nevski²⁵, F.M. Newcomer¹²⁰, P.R. Newman¹⁸, V. Nguyen Thi Hong¹³⁶, R.B. Nickerson¹¹⁸, R. Nicolaïdou¹³⁶, B. Nicquevert³⁰, F. Niedercorn¹¹⁵, J. Nielsen¹³⁷, N. Nikiforou³⁵, A. Nikiforov¹⁶, V. Nikolaenko¹²⁸, I. Nikolic-Audit⁷⁸, K. Nikolics⁴⁹, K. Nikolopoulos¹⁸, H. Nilsen⁴⁸, P. Nilsson⁸, Y. Ninomiya¹⁵⁵, A. Nisati^{132a}, R. Nisius⁹⁹, T. Nobe¹⁵⁷, L. Nodulman⁶, M. Nomachi¹¹⁶, I. Nomidis¹⁵⁴, S. Norberg¹¹¹, M. Nordberg³⁰, P.R. Norton¹²⁹, J. Novakova¹²⁶, M. Nozaki⁶⁵, L. Nozka¹¹³, I.M. Nugent^{159a}, A.-E. Nuncio-Quiroz²¹, G. Nunes Hanninger⁸⁶, T. Nunnemann⁹⁸, E. Nurse⁷⁷, B.J. O'Brien⁴⁶, S.W. O'Neale^{18,*}, D.C. O'Neil¹⁴², V. O'Shea⁵³, L.B. Oakes⁹⁸, F.G. Oakham^{29,d}, H. Oberlack⁹⁹, J. Ocariz⁷⁸, A. Ochi⁶⁶, S. Oda⁶⁹, S. Odaka⁶⁵, J. Odier⁸³, H. Ogren⁶⁰, A. Oh⁸², S.H. Oh⁴⁵, C.C. Ohm³⁰, T. Ohshima¹⁰¹, H. Okawa²⁵, Y. Okumura³¹, T. Okuyama¹⁵⁵, A. Olariu^{26a}, A.G. Olchevski⁶⁴, S.A. Olivares Pino^{32a}, M. Oliveira^{124a,h}, D. Oliveira Damazio²⁵, E. Oliver Garcia¹⁶⁷, D. Olivito¹²⁰, A. Olszewski³⁹, J. Olszowska³⁹, A. Onofre^{124a,ab}, P.U.E. Onyisi³¹, C.J. Oram^{159a}, M.J. Oreiglia³¹, Y. Oren¹⁵³, D. Orestano^{134a,134b}, N. Orlando^{72a,72b}, I. Orlov¹⁰⁷, C. Oropeza Barrera⁵³, R.S. Orr¹⁵⁸, B. Osculati^{50a,50b}, R. Ospanov¹²⁰, C. Osuna¹², G. Otero y Garzon²⁷, J.P. Ottersbach¹⁰⁵, M. Ouchrif^{135d}, E.A. Ouellette¹⁶⁹, F. Ould-Saada¹¹⁷, A. Ouraou¹³⁶, Q. Ouyang^{33a}, A. Ovcharova¹⁵, M. Owen⁸², S. Owen¹³⁹, V.E. Ozcan^{19a}, N. Ozturk⁸, A. Pacheco Pages¹², C. Padilla Aranda¹², S. Pagan Griso¹⁵, E. Paganis¹³⁹, C. Pahl⁹⁹, F. Paige²⁵, P. Pais⁸⁴, K. Pajchel¹¹⁷, G. Palacino^{159b}, C.P. Paleari⁷, S. Palestini³⁰, D. Pallin³⁴, A. Palma^{124a}, J.D. Palmer¹⁸, Y.B. Pan¹⁷³, E. Panagiotopoulou¹⁰, P. Pani¹⁰⁵, N. Panikashvili⁸⁷, S. Panitkin²⁵, D. Pantea^{26a}, A. Papadelis^{146a}, Th.D. Papadopoulou¹⁰, A. Paramonov⁶, D. Paredes Hernandez³⁴, W. Park^{25,ac}, M.A. Parker²⁸, F. Parodi^{50a,50b}, J.A. Parsons³⁵, U. Parzefall⁴⁸, S. Pashapour⁵⁴, E. Pasqualucci^{132a}, S. Passaggio^{50a}, A. Passeri^{134a}, F. Pastore^{134a,134b,*}, Fr. Pastore⁷⁶, G. Pásztor^{49,ad}, S. Pataraia¹⁷⁵, N. Patel¹⁵⁰, J.R. Pater⁸², S. Patricelli^{102a,102b}, T. Pauly³⁰, M. Pecs^{144a}, S. Pedraza Lopez¹⁶⁷, M.I. Pedraza Morales¹⁷³, S.V. Peleganchuk¹⁰⁷, D. Pelikan¹⁶⁶, H. Peng^{33b}, B. Penning³¹, A. Penson³⁵, J. Penwell⁶⁰, M. Perantoni^{24a}, K. Perez^{35,ae}, T. Perez Cavalcanti⁴², E. Perez Codina^{159a}, M.T. Pérez García-Estañ¹⁶⁷, V. Perez Reale³⁵, L. Perini^{89a,89b}, H. Pernegger³⁰, R. Perrino^{72a}, P. Perodo⁵, V.D. Peshekhanov⁶⁴, K. Peters³⁰, B.A. Petersen³⁰, J. Petersen³⁰, T.C. Petersen³⁶, E. Petit⁵, A. Petridis¹⁵⁴, C. Petridou¹⁵⁴, E. Petrolo^{132a}, F. Petrucci^{134a,134b}, D. Petschull⁴², M. Petteni¹⁴², R. Pezoa^{32b}, A. Phan⁸⁶, P.W. Phillips¹²⁹, G. Pi-acquadro³⁰, A. Picazio⁴⁹, E. Piccaro⁷⁵, M. Piccinini^{20a,20b}, S.M. Piec⁴², R. Piegaia²⁷, D.T. Pignotti¹⁰⁹, J.E. Pilcher³¹, A.D. Pilkington⁸², J. Pina^{124a,b}, M. Pinamonti^{164a,164c}, A. Pinder¹¹⁸, J.L. Pinfold³, B. Pinto^{124a}, C. Pizio^{89a,89b}, M. Plamondon¹⁶⁹, M.-A. Pleier²⁵, E. Plotnikova⁶⁴, A. Poblaguev²⁵, S. Poddar^{58a}, F. Podlaski³⁴, L. Poggiali¹¹⁵, D. Pohl²¹, M. Pohl⁴⁹, G. Polesello^{119a}, A. Pollicchio^{37a,37b}, A. Polini^{20a}, J. Poll⁷⁵, V. Polychronakos²⁵, D. Pomeroy²³, K. Pommès³⁰, L. Pontecorvo^{132a}, B.G. Pope⁸⁸, G.A. Popenciu^{26a}, D.S. Popovic^{13a}, A. Poppleton³⁰, X. Portell Bueso³⁰, G.E. Pospelov⁹⁹, S. Pospisil¹²⁷, I.N. Potrap⁹⁹, C.J. Potter¹⁴⁹, C.T. Potter¹¹⁴, G. Poulard³⁰, J. Poveda⁶⁰, V. Pozdnyakov⁶⁴, R. Prabhu⁷⁷, P. Pralavorio⁸³, A. Pranko¹⁵, S. Prasad³⁰, R. Pravahan²⁵, S. Prell⁶³, K. Pretzl¹⁷, D. Price⁶⁰, J. Price⁷³, L.E. Price⁶, D. Prieur¹²³, M. Primavera^{72a}, K. Prokofiev¹⁰⁸, F. Prokoshin^{32b}, S. Protopopescu²⁵, J. Proudfoot⁶, X. Prudent⁴⁴, M. Przybycien³⁸, H. Przysiezniak⁵, S. Psoroulas²¹, E. Ptacek¹¹⁴, E. Puesche⁸⁴, J. Purdham⁸⁷, M. Purohit^{25,ac}, P. Puzo¹¹⁵, Y. Pylyphenko⁶², J. Qian⁸⁷, A. Quadt⁵⁴, D.R. Quarrie¹⁵, W.B. Quayle¹⁷³, F. Quinonez^{32a}, M. Raas¹⁰⁴, V. Radeka²⁵, V. Radescu⁴², P. Radloff¹¹⁴, T. Rador^{19a}, F. Ragusa^{89a,89b}, G. Rahal¹⁷⁸, A.M. Rahimi¹⁰⁹, D. Rahm²⁵, S. Rajagopalan²⁵, M. Rammensee⁴⁸, M. Rammes¹⁴¹, A.S. Randle-Conde⁴⁰, K. Randrianarivony²⁹, F. Rauscher⁹⁸, T.C. Rave⁴⁸, M. Raymond³⁰, A.L. Read¹¹⁷, D.M. Rebuzzi^{119a,119b}, A. Redelbach¹⁷⁴, G. Redlinger²⁵, R. Reece¹²⁰, K. Reeves⁴¹, E. Reinherz-Aronis¹⁵³, A. Reinsch¹¹⁴, I. Reisinger⁴³, C. Rembser³⁰, Z.L. Ren¹⁵¹, A. Renaud¹¹⁵, M. Rescigno^{132a}, S. Resconi^{89a}, B. Resende¹³⁶, P. Reznicek⁹⁸, R. Rezvani¹⁵⁸, R. Richter⁹⁹, E. Richter-Was^{5,af}, M. Ridel⁷⁸, M. Rijpstra¹⁰⁵, M. Rijssenbeek¹⁴⁸, A. Rimoldi^{119a,119b}, L. Rinaldi^{20a}, R.R. Rios⁴⁰, I. Riu¹², G. Rivoltella^{89a,89b}, F. Rizatdinova¹¹², E. Rizvi⁷⁵, S.H. Robertson^{85,k}, A. Robichaud-Veronneau¹¹⁸, D. Robinson²⁸, J.E.M. Robinson⁸², A. Robson⁵³, J.G. Rocha de Lima¹⁰⁶, C. Roda^{122a,122b}, D. Roda Dos Santos³⁰, A. Roe⁵⁴, S. Roe³⁰, O. Røhne¹¹⁷, S. Rolli¹⁶¹, A. Romaniouk⁹⁶, M. Romano^{20a,20b}, G. Romeo²⁷, E. Romero Adam¹⁶⁷, N. Rompotis¹³⁸, L. Roos⁷⁸, E. Ros¹⁶⁷, S. Rosati^{132a}, K. Rosbach⁴⁹, A. Rose¹⁴⁹, M. Rose⁷⁶, G.A. Rosenbaum¹⁵⁸, E.I. Rosenberg⁶³, PL. Rosendahl¹⁴, O. Rosenthal¹⁴¹, L. Rosselet⁴⁹, V. Rossetti¹², E. Rossi^{132a,132b}, L.P. Rossi^{50a}, M. Rotaru^{26a}, I. Roth¹⁷², J. Rothberg¹³⁸, D. Rousseau¹¹⁵, C.R. Royon¹³⁶, A. Rozanov⁸³, Y. Rozen¹⁵², X. Ruan^{33a,ag}, F. Rubbo¹², I. Rubinskiy⁴², N. Ruckstuhl¹⁰⁵, V.I. Rud⁹⁷, C. Rudolph⁴⁴, G. Rudolph⁶¹, F. Rühr⁷, A. Ruiz-Martinez⁶³, L. Rumyantsev⁶⁴, Z. Rurikova⁴⁸, N.A. Rusakovich⁶⁴, J.P. Rutherford⁷, C. Ruwiedel^{15,*}, P. Ruzicka¹²⁵, Y.F. Ryabov¹²¹,

- M. Rybar¹²⁶, G. Rybkin¹¹⁵, N.C. Ryder¹¹⁸, A.F. Saavedra¹⁵⁰, I. Sadeh¹⁵³, H.F-W. Sadrozinski¹³⁷, R. Sadykov⁶⁴, F. Safai Tehrani^{132a}, H. Sakamoto¹⁵⁵, G. Salamanna⁷⁵, A. Salamon^{133a}, M. Saleem¹¹¹, D. Salek³⁰, D. Salihagic⁹⁹, A. Salnikov¹⁴³, J. Salt¹⁶⁷, B.M. Salvachua Ferrando⁶, D. Salvatore^{37a,37b}, F. Salvatore¹⁴⁹, A. Salvucci¹⁰⁴, A. Salzburger³⁰, D. Sampsonidis¹⁵⁴, B.H. Samset¹¹⁷, A. Sanchez^{102a,102b}, V. Sanchez Martinez¹⁶⁷, H. Sandaker¹⁴, H.G. Sander⁸¹, M.P. Sanders⁹⁸, M. Sandhoff¹⁷⁵, T. Sandoval²⁸, C. Sandoval¹⁶², R. Sandstroem⁹⁹, D.P.C. Sankey¹²⁹, A. Sansoni⁴⁷, C. Santamarina Rios⁸⁵, C. Santoni³⁴, R. Santonico^{133a,133b}, H. Santos^{124a}, J.G. Saraiva^{124a}, T. Sarangi¹⁷³, E. Sarkisyan-Grinbaum⁸, F. Sarri^{122a,122b}, G. Sartisohn¹⁷⁵, O. Sasaki⁶⁵, Y. Sasaki¹⁵⁵, N. Sasao⁶⁷, I. Satsounkevitch⁹⁰, G. Sauvage^{5,*}, E. Sauvan⁵, J.B. Sauvan¹¹⁵, P. Savard^{158,d}, V. Savinov¹²³, D.O. Savu³⁰, L. Sawyer^{25,m}, D.H. Saxon⁵³, J. Saxon¹²⁰, C. Sbarra^{20a}, A. Sbrizzi^{20a,20b}, D.A. Scannicchio¹⁶³, M. Scarcella¹⁵⁰, J. Schaarschmidt¹¹⁵, P. Schacht⁹⁹, D. Schaefer¹²⁰, U. Schäfer⁸¹, S. Schaepe²¹, S. Schaezel^{58b}, A.C. Schaffer¹¹⁵, D. Schaile⁹⁸, R.D. Schamberger¹⁴⁸, A.G. Schamov¹⁰⁷, V. Scharf^{58a}, V.A. Schegelsky¹²¹, D. Scheirich⁸⁷, M. Schernau¹⁶³, M.I. Scherzer³⁵, C. Schiavi^{50a,50b}, J. Schieck⁹⁸, M. Schioppa^{37a,37b}, S. Schlenker³⁰, E. Schmidt⁴⁸, K. Schmieden²¹, C. Schmitt⁸¹, S. Schmitt^{58b}, M. Schmitz²¹, B. Schneider¹⁷, U. Schnoor⁴⁴, A. Schoening^{58b}, A.L.S. Schorlemmer⁵⁴, M. Schott³⁰, D. Schouten^{159a}, J. Schovancova¹²⁵, M. Schram⁸⁵, C. Schroeder⁸¹, N. Schroer^{58c}, M.J. Schultens²¹, J. Schultes¹⁷⁵, H.-C. Schultz-Coulon^{58a}, H. Schulz¹⁶, M. Schumacher⁴⁸, B.A. Schumm¹³⁷, Ph. Schune¹³⁶, C. Schwanenberger⁸², A. Schwartzman¹⁴³, Ph. Schwegler⁹⁹, Ph. Schwemling⁷⁸, R. Schwienhorst⁸⁸, R. Schwierz⁴⁴, J. Schwindling¹³⁶, T. Schwindt²¹, M. Schwoerer⁵, G. Sciolla²³, W.G. Scott¹²⁹, J. Searcy¹¹⁴, G. Sedov⁴², E. Sedykh¹²¹, S.C. Seidel¹⁰³, A. Seiden¹³⁷, F. Seifert⁴⁴, J.M. Seixas^{24a}, G. Sekhniaidze^{102a}, S.J. Sekula⁴⁰, K.E. Selbach⁴⁶, D.M. Seliverstov¹²¹, B. Sellden^{146a}, G. Sellers⁷³, M. Seman^{144b}, N. Semprini-Cesarini^{20a,20b}, C. Serfon⁹⁸, L. Serin¹¹⁵, L. Serkin⁵⁴, R. Seuster⁹⁹, H. Severini¹¹¹, A. Sfyrla³⁰, E. Shabalina⁵⁴, M. Shamim¹¹⁴, L.Y. Shan^{33a}, J.T. Shank²², Q.T. Shao⁸⁶, M. Shapiro¹⁵, P.B. Shatalov⁹⁵, K. Shaw^{164a,164c}, D. Sherman¹⁷⁶, P. Sherwood⁷⁷, A. Shibata¹⁰⁸, S. Shimizu¹⁰¹, M. Shimojima¹⁰⁰, T. Shin⁵⁶, M. Shiyakova⁶⁴, A. Shmeleva⁹⁴, M.J. Shochet³¹, D. Short¹¹⁸, S. Shrestha⁶³, E. Shulga⁹⁶, M.A. Shupe⁷, P. Sicho¹²⁵, A. Sidoti^{132a}, F. Siegert⁴⁸, Dj. Sijacki^{13a}, O. Silbert¹⁷², J. Silva^{124a}, Y. Silver¹⁵³, D. Silverstein¹⁴³, S.B. Silverstein^{146a}, V. Simak¹²⁷, O. Simard¹³⁶, Lj. Simic^{13a}, S. Simion¹¹⁵, E. Simioni⁸¹, B. Simmons⁷⁷, R. Simonello^{89a,89b}, M. Simonyan³⁶, P. Sinervo¹⁵⁸, N.B. Sinev¹¹⁴, V. Sipica¹⁴¹, G. Siragusa¹⁷⁴, A. Sircar²⁵, A.N. Sisakyan^{64,*}, S.Yu. Sivoklokov⁹⁷, J. Sjölin^{146a,146b}, T.B. Sjursen¹⁴, L.A. Skinnari¹⁵, H.P. Skottowe⁵⁷, K. Skovpen¹⁰⁷, P. Skubic¹¹¹, M. Slater¹⁸, T. Slavicek¹²⁷, K. Sliwa¹⁶¹, V. Smakhtin¹⁷², B.H. Smart⁴⁶, S.Yu. Smirnov⁹⁶, Y. Smirnov⁹⁶, L.N. Smirnova⁹⁷, O. Smirnova⁷⁹, B.C. Smith⁵⁷, D. Smith¹⁴³, K.M. Smith⁵³, M. Smizanska⁷¹, K. Smolek¹²⁷, A.A. Snesarev⁹⁴, S.W. Snow⁸², J. Snow¹¹¹, S. Snyder²⁵, R. Sobie^{169,k}, J. Sodomka¹²⁷, A. Soffer¹⁵³, C.A. Solans¹⁶⁷, M. Solar¹²⁷, J. Solc¹²⁷, E.Yu. Soldatov⁹⁶, U. Soldevila¹⁶⁷, E. Solfaroli Camillocci^{132a,132b}, A.A. Solodkov¹²⁸, O.V. Solovyanov¹²⁸, V. Solov'yev¹²¹, N. Soni¹, V. Sopko¹²⁷, B. Sopko¹²⁷, M. Sosebee⁸, R. Soualah^{164a,164c}, A. Soukharev¹⁰⁷, S. Spagnolo^{72a,72b}, F. Spanò⁷⁶, R. Spighi^{20a}, G. Spigo³⁰, R. Spiwoks³⁰, M. Spousta^{126,ah}, T. Spreitzer¹⁵⁸, B. Spurlock⁸, R.D. St. Denis⁵³, J. Stahlman¹²⁰, R. Stamen^{58a}, E. Stancka³⁹, R.W. Stanek⁶, C. Stanescu^{134a}, M. Stanescu-Bellu⁴², S. Stapnes¹¹⁷, E.A. Starchenko¹²⁸, J. Stark⁵⁵, P. Staroba¹²⁵, P. Starovoitov⁴², R. Staszewski³⁹, A. Staude⁹⁸, P. Stavina^{144a,*}, G. Steele⁵³, P. Steinbach⁴⁴, P. Steinberg²⁵, I. Stekl¹²⁷, B. Stelzer¹⁴², H.J. Stelzer⁸⁸, O. Stelzer-Chilton^{159a}, H. Stenzel⁵², S. Stern⁹⁹, G.A. Stewart³⁰, J.A. Stillings²¹, M.C. Stockton⁸⁵, K. Stoerig⁴⁸, G. Stoica^{26a}, S. Stonjek⁹⁹, P. Strachota¹²⁶, A.R. Stradling⁸, A. Straessner⁴⁴, J. Strandberg¹⁴⁷, S. Strandberg^{146a,146b}, A. Strandlie¹¹⁷, M. Strang¹⁰⁹, E. Strauss¹⁴³, M. Strauss¹¹¹, P. Strizenec^{144b}, R. Ströhmer¹⁷⁴, D.M. Strom¹¹⁴, J.A. Strong^{76,*}, R. Stroynowski⁴⁰, J. Strube¹²⁹, B. Stugu¹⁴, I. Stumer^{25,*}, J. Stupak¹⁴⁸, P. Sturm¹⁷⁵, N.A. Styles⁴², D.A. Soh^{151,w}, D. Su¹⁴³, HS. Subramania³, A. Succurro¹², Y. Sugaya¹¹⁶, C. Suhr¹⁰⁶, M. Suk¹²⁶, V.V. Sulin⁹⁴, S. Sultansoy^{4d}, T. Sumida⁶⁷, X. Sun⁵⁵, J.E. Sundermann⁴⁸, K. Suruliz¹³⁹, G. Susinno^{37a,37b}, M.R. Sutton¹⁴⁹, Y. Suzuki⁶⁵, Y. Suzuki⁶⁶, M. Svatos¹²⁵, S. Swedish¹⁶⁸, I. Sykora^{144a}, T. Sykora¹²⁶, J. Sánchez¹⁶⁷, D. Ta¹⁰⁵, K. Tackmann⁴², A. Taf-fard¹⁶³, R. Tafirout^{159a}, N. Taiblum¹⁵³, Y. Takahashi¹⁰¹, H. Takai²⁵, R. Takashima⁶⁸, H. Takeda⁶⁶, T. Takeshita¹⁴⁰, Y. Takubo⁶⁵, M. Talby⁸³, A. Talyshев^{107,f}, M.C. Tamsett²⁵, K.G. Tan⁸⁶, J. Tanaka¹⁵⁵, R. Tanaka¹¹⁵, S. Tanaka¹³¹, S. Tanaka⁶⁵, A.J. Tanasiyczuk¹⁴², K. Tani⁶⁶, N. Tannoury⁸³, S. Tapprogge⁸¹, D. Tardif¹⁵⁸, S. Tarem¹⁵², F. Tarrade²⁹, G.F. Tartarelli^{89a}, P. Tas¹²⁶, M. Tasevsky¹²⁵, E. Tassi^{37a,37b}, M. Tatarkhanov¹⁵, Y. Tayalati^{135d}, C. Taylor⁷⁷, F.E. Taylor⁹², G.N. Taylor⁸⁶, W. Taylor^{159b}, M. Teinturier¹¹⁵, F.A. Teischinger³⁰, M. Teixeira Dias Castanheira⁷⁵, P. Teixeira-Dias⁷⁶, K.K. Temming⁴⁸, H. Ten Kate³⁰, P.K. Teng¹⁵¹, S. Terada⁶⁵, K. Terashi¹⁵⁵, J. Terron⁸⁰, M. Testa⁴⁷, R.J. Teuscher^{158,k}, J. Therhaag²¹, T. Theveneaux-Pelzer⁷⁸, S. Thoma⁴⁸, J.P. Thomas¹⁸, E.N. Thompson³⁵, P.D. Thompson¹⁸, P.D. Thompson¹⁵⁸, A.S. Thompson⁵³, L.A. Thomsen³⁶, E. Thomson¹²⁰, M. Thomson²⁸, W.M. Thong⁸⁶, R.P. Thun⁸⁷, F. Tian³⁵, M.J. Tibbetts¹⁵, T. Tic¹²⁵, V.O. Tikhomirov⁹⁴, Y.A. Tikhonov^{107,f}, S. Timoshenko⁹⁶, P. Tipton¹⁷⁶, S. Tisserant⁸³, T. Todorov⁵, S. Todorova-Nova¹⁶¹, B. Toggerson¹⁶³, J. Tojo⁶⁹, S. Tokár^{144a}, K. Tokushuku⁶⁵, K. Tolleson⁸⁸, M. Tomoto¹⁰¹, L. Tompkins³¹, K. Toms¹⁰³, A. Tonoyan¹⁴, C. Topfel¹⁷, N.D. Topilin⁶⁴, I. Torchiani³⁰, E. Torrence¹¹⁴, H. Torres⁷⁸, E. Torró Pastor¹⁶⁷, J. Toth^{83,ad}, F. Touchard⁸³, D.R. Tovey¹³⁹, T. Trefzger¹⁷⁴, L. Tremblet³⁰, A. Tricoli³⁰, I.M. Trigger^{159a}, S. Trincasz-Duvoud⁷⁸, M.F. Tripiana⁷⁰, N. Triplett²⁵, W. Trischuk¹⁵⁸, B. Trocmé⁵⁵, C. Troncon^{89a}, M. Trottier-McDonald¹⁴², M. Trze-

binski³⁹, A. Trzupek³⁹, C. Tsarouchas³⁰, J.C-L. Tseng¹¹⁸, M. Tsiakiris¹⁰⁵, P.V. Tsiareshka⁹⁰, D. Tsionou^{5,ai}, G. Tsipolitis¹⁰, S. Tsiskaridze¹², V. Tsiskaridze⁴⁸, E.G. Tskhadadze^{51a}, I.I. Tsukerman⁹⁵, V. Tsulaia¹⁵, J.-W. Tsung²¹, S. Tsuno⁶⁵, D. Tsybychev¹⁴⁸, A. Tua¹³⁹, A. Tudorache^{26a}, V. Tudorache^{26a}, J.M. Tuggle³¹, M. Turala³⁹, D. Turecek¹²⁷, I. Turk Cakir^{4e}, E. Turlay¹⁰⁵, R. Turra^{89a,89b}, P.M. Tuts³⁵, A. Tykhonov⁷⁴, M. Tylmad^{146a,146b}, M. Tyndel¹²⁹, G. Tzanakos⁹, K. Uchida²¹, I. Ueda¹⁵⁵, R. Ueno²⁹, M. Ugland¹⁴, M. Uhlenbrock²¹, M. Uhrmacher⁵⁴, F. Ukegawa¹⁶⁰, G. Unal³⁰, A. Undrus²⁵, G. Une¹⁶³, Y. Unno⁶⁵, D. Urbaniec³⁵, G. Usai⁸, M. Uslenghi^{119a,119b}, L. Vacavant⁸³, V. Vacek¹²⁷, B. Vachon⁸⁵, S. Vahsen¹⁵, J. Valenta¹²⁵, S. Valentinetto^{20a,20b}, A. Valero¹⁶⁷, S. Valkar¹²⁶, E. Valladolid Gallego¹⁶⁷, S. Vallecorsa¹⁵², J.A. Valls Ferrer¹⁶⁷, R. Van Berg¹²⁰, P.C. Van Der Deijl¹⁰⁵, R. van der Geer¹⁰⁵, H. van der Graaf¹⁰⁵, R. Van Der Leeuw¹⁰⁵, E. van der Poel¹⁰⁵, D. van der Ster³⁰, N. van Eldik³⁰, P. van Gemmeren⁶, I. van Vulpen¹⁰⁵, M. Vanadia⁹⁹, W. Vandelli³⁰, A. Vaniachine⁶, P. Vankov⁴², F. Vannucci⁷⁸, R. Vari^{132a}, T. Varol⁸⁴, D. Varouchas¹⁵, A. Vartapetian⁸, K.E. Varvell¹⁵⁰, V.I. Vassilakopoulos⁵⁶, F. Vazeille³⁴, T. Vazquez Schroeder⁵⁴, G. Vegni^{89a,89b}, J.J. Veillet¹¹⁵, F. Veloso^{124a}, R. Veness³⁰, S. Veneziano^{132a}, A. Ventura^{72a,72b}, D. Ventura⁸⁴, M. Venturi⁴⁸, N. Venturi¹⁵⁸, V. Vercesi^{119a}, M. Verducci¹³⁸, W. Verkerke¹⁰⁵, J.C. Vermeulen¹⁰⁵, A. Vest⁴⁴, M.C. Vetterli^{142,d}, I. Vichou¹⁶⁵, T. Vickey^{145b,aj}, O.E. Vickey Boeriu^{145b}, G.H.A. Viehhauser¹¹⁸, S. Viel¹⁶⁸, M. Villa^{20a,20b}, M. Villaplana Perez¹⁶⁷, E. Vilucchi⁴⁷, M.G. Vincter²⁹, E. Vinek³⁰, V.B. Vinogradov⁶⁴, M. Virchaux^{136,*}, J. Virzì¹⁵, O. Vitells¹⁷², M. Vitti⁴², I. Vivarelli⁴⁸, F. Vives Vaque³, S. Vlachos¹⁰, D. Vladoiu⁹⁸, M. Vlasak¹²⁷, A. Vogel²¹, P. Vokac¹²⁷, G. Volpi⁴⁷, M. Volpi⁸⁶, G. Volpini^{89a}, H. von der Schmitt⁹⁹, H. von Radziewski⁴⁸, E. von Toerne²¹, V. Vorobel¹²⁶, V. Vorwerk¹², M. Vos¹⁶⁷, R. Voss³⁰, T.T. Voss¹⁷⁵, J.H. Vossebeld⁷³, N. Vranjes¹³⁶, M. Vranjes Milosavljevic¹⁰⁵, V. Vrba¹²⁵, M. Vreeswijk¹⁰⁵, T. Vu Anh⁴⁸, R. Vuillermet³⁰, I. Vukotic³¹, W. Wagner¹⁷⁵, P. Wagner¹²⁰, H. Wahlen¹⁷⁵, S. Wahrmund⁴⁴, J. Wakabayashi¹⁰¹, S. Walch⁸⁷, J. Walder⁷¹, R. Walker⁹⁸, W. Walkowiak¹⁴¹, R. Wall¹⁷⁶, P. Waller⁷³, B. Walsh¹⁷⁶, C. Wang⁴⁵, H. Wang¹⁷³, H. Wang^{33b,ak}, J. Wang¹⁵¹, J. Wang⁵⁵, R. Wang¹⁰³, S.M. Wang¹⁵¹, T. Wang²¹, A. Warburton⁸⁵, C.P. Ward²⁸, M. Warsinsky⁴⁸, A. Washbrook⁴⁶, C. Wasicki⁴², I. Watanabe⁶⁶, P.M. Watkins¹⁸, A.T. Watson¹⁸, I.J. Watson¹⁵⁰, M.F. Watson¹⁸, G. Watts¹³⁸, S. Watts⁸², A.T. Waugh¹⁵⁰, B.M. Waugh⁷⁷, M.S. Weber¹⁷, P. Weber⁵⁴, A.R. Weidberg¹¹⁸, P. Weigell⁹⁹, J. Weingarten⁵⁴, C. Weiser⁴⁸, H. Wellenstein²³, P.S. Wells³⁰, T. Wenaus²⁵, D. Wendland¹⁶, Z. Weng^{151,w}, T. Wengler³⁰, S. Wenig³⁰, N. Wermes²¹, M. Werner⁴⁸, P. Werner³⁰, M. Werth¹⁶³, M. Wessels^{58a}, J. Wetter¹⁶¹, C. Weydert⁵⁵, K. Whalen²⁹, S.J. Wheeler-Ellis¹⁶³, A. White⁸, M.J. White⁸⁶, S. White^{122a,122b}, S.R. Whitehead¹¹⁸, D. Whiteson¹⁶³, D. Whittington⁶⁰, F. Wicek¹¹⁵, D. Wicke¹⁷⁵, F.J. Wickens¹²⁹, W. Wiedenmann¹⁷³, M. Wielers¹²⁹, P. Wienemann²¹, C. Wiglesworth⁷⁵, L.A.M. Wiik-Fuchs⁴⁸, P.A. Wijeratne⁷⁷, A. Wildauer⁹⁹, M.A. Wildt^{42,s}, I. Wilhelm¹²⁶, H.G. Wilkens³⁰, J.Z. Will⁹⁸, E. Williams³⁵, H.H. Williams¹²⁰, W. Willis³⁵, S. Willocq⁸⁴, J.A. Wilson¹⁸, M.G. Wilson¹⁴³, A. Wilson⁸⁷, I. Wingerter-Seez⁵, S. Winkelmann⁴⁸, F. Winklmeier³⁰, M. Wittgen¹⁴³, S.J. Wollstadt⁸¹, M.W. Wolter³⁹, H. Wolters^{124a,h}, W.C. Wong⁴¹, G. Wooden⁸⁷, B.K. Wosiek³⁹, J. Wotschack³⁰, M.J. Woudstra⁸², K.W. Wozniak³⁹, K. Wraight⁵³, M. Wright⁵³, B. Wrona⁷³, S.L. Wu¹⁷³, X. Wu⁴⁹, Y. Wu^{33b,al}, E. Wulf³⁵, B.M. Wynne⁴⁶, S. Xella³⁶, M. Xiao¹³⁶, S. Xie⁴⁸, C. Xu^{33b,z}, D. Xu¹³⁹, B. Yabsley¹⁵⁰, S. Yacoob^{145a,am}, M. Yamada⁶⁵, H. Yamaguchi¹⁵⁵, A. Yamamoto⁶⁵, K. Yamamoto⁶³, S. Yamamoto¹⁵⁵, T. Yamamura¹⁵⁵, T. Yamanaka¹⁵⁵, J. Yamaoka⁴⁵, T. Yamazaki¹⁵⁵, Y. Yamazaki⁶⁶, Z. Yan²², H. Yang⁸⁷, U.K. Yang⁸², Y. Yang⁶⁰, Z. Yang^{146a,146b}, S. Yanush⁹¹, L. Yao^{33a}, Y. Yao¹⁵, Y. Yasu⁶⁵, G.V. Ybeles Smit¹³⁰, J. Ye⁴⁰, S. Ye²⁵, M. Yilmaz^{4c}, R. Yoosoofmiya¹²³, K. Yorita¹⁷¹, R. Yoshida⁶, C. Young¹⁴³, C.J. Young¹¹⁸, S. Youssef²², D. Yu²⁵, J. Yu⁸, J. Yu¹¹², L. Yuan⁶⁶, A. Yurkewicz¹⁰⁶, M. Byszewski³⁰, B. Zabinski³⁹, R. Zaidan⁶², A.M. Zaitsev¹²⁸, Z. Zajacova³⁰, L. Zanello^{132a,132b}, D. Zanzi⁹⁹, A. Zaytsev²⁵, C. Zeitnitz¹⁷⁵, M. Zeman¹²⁵, A. Zemla³⁹, C. Zendler²¹, O. Zenin¹²⁸, T. Ženiš^{144a}, Z. Zinonos^{122a,122b}, S. Zenz¹⁵, D. Zerwas¹¹⁵, G. Zevi della Porta⁵⁷, Z. Zhan^{33d}, D. Zhang^{33b,ak}, H. Zhang⁸⁸, J. Zhang⁶, X. Zhang^{33d}, Z. Zhang¹¹⁵, L. Zhao¹⁰⁸, T. Zhao¹³⁸, Z. Zhao^{33b}, A. Zhemchugov⁶⁴, J. Zhong¹¹⁸, B. Zhou⁸⁷, N. Zhou¹⁶³, Y. Zhou¹⁵¹, C.G. Zhu^{33d}, H. Zhu⁴², J. Zhu⁸⁷, Y. Zhu^{33b}, X. Zhuang⁹⁸, V. Zhuravlov⁹⁹, D. Ziemińska⁶⁰, N.I. Zimin⁶⁴, R. Zimmermann²¹, S. Zimmermann²¹, S. Zimmermann⁴⁸, M. Ziolkowski¹⁴¹, R. Zitoun⁵, L. Živković³⁵, V.V. Zmouchko^{128,*}, G. Zobernig¹⁷³, A. Zoccoli^{20a,20b}, M. zur Nedden¹⁶, V. Zutshi¹⁰⁶, L. Zwalski³⁰

¹School of Chemistry and Physics, University of Adelaide, Adelaide, Australia²Physics Department, SUNY Albany, Albany NY, United States of America³Department of Physics, University of Alberta, Edmonton AB, Canada^{4(a)}Department of Physics, Ankara University, Ankara; ^(b)Department of Physics, Dumluipinar University, Kutahya;^(c)Department of Physics, Gazi University, Ankara; ^(d)Division of Physics, TOBB University of Economics and Technology, Ankara; ^(e)Turkish Atomic Energy Authority, Ankara, Turkey⁵LAPP, CNRS/IN2P3 and Université de Savoie, Annecy-le-Vieux, France⁶High Energy Physics Division, Argonne National Laboratory, Argonne IL, United States of America⁷Department of Physics, University of Arizona, Tucson AZ, United States of America⁸Department of Physics, The University of Texas at Arlington, Arlington TX, United States of America⁹Physics Department, University of Athens, Athens, Greece

- ¹⁰Physics Department, National Technical University of Athens, Zografou, Greece
¹¹Institute of Physics, Azerbaijan Academy of Sciences, Baku, Azerbaijan
¹²Institut de Física d'Altes Energies and Departament de Física de la Universitat Autònoma de Barcelona and ICREA, Barcelona, Spain
¹³(a) Institute of Physics, University of Belgrade, Belgrade; (b) Vinca Institute of Nuclear Sciences, University of Belgrade, Belgrade, Serbia
¹⁴Department for Physics and Technology, University of Bergen, Bergen, Norway
¹⁵Physics Division, Lawrence Berkeley National Laboratory and University of California, Berkeley CA, United States of America
¹⁶Department of Physics, Humboldt University, Berlin, Germany
¹⁷Albert Einstein Center for Fundamental Physics and Laboratory for High Energy Physics, University of Bern, Bern, Switzerland
¹⁸School of Physics and Astronomy, University of Birmingham, Birmingham, United Kingdom
¹⁹(a) Department of Physics, Bogazici University, Istanbul; (b) Division of Physics, Dogus University, Istanbul;
(c) Department of Physics Engineering, Gaziantep University, Gaziantep; (d) Department of Physics, Istanbul Technical University, Istanbul, Turkey
²⁰(a) INFN Sezione di Bologna; (b) Dipartimento di Fisica, Università di Bologna, Bologna, Italy
²¹Physikalischs Institut, University of Bonn, Bonn, Germany
²²Department of Physics, Boston University, Boston MA, United States of America
²³Department of Physics, Brandeis University, Waltham MA, United States of America
²⁴(a) Universidade Federal do Rio De Janeiro COPPE/EE/IF, Rio de Janeiro; (b) Federal University of Juiz de Fora (UFJF), Juiz de Fora; (c) Federal University of Sao Joao del Rei (UFSJ), Sao Joao del Rei; (d) Instituto de Fisica, Universidade de Sao Paulo, Sao Paulo, Brazil
²⁵Physics Department, Brookhaven National Laboratory, Upton NY, United States of America
²⁶(a) National Institute of Physics and Nuclear Engineering, Bucharest; (b) University Politehnica Bucharest, Bucharest;
(c) West University in Timisoara, Timisoara, Romania
²⁷Departamento de Física, Universidad de Buenos Aires, Buenos Aires, Argentina
²⁸Cavendish Laboratory, University of Cambridge, Cambridge, United Kingdom
²⁹Department of Physics, Carleton University, Ottawa ON, Canada
³⁰CERN, Geneva, Switzerland
³¹Enrico Fermi Institute, University of Chicago, Chicago IL, United States of America
³²(a) Departamento de Física, Pontificia Universidad Católica de Chile, Santiago; (b) Departamento de Física, Universidad Técnica Federico Santa María, Valparaíso, Chile
³³(a) Institute of High Energy Physics, Chinese Academy of Sciences, Beijing; (b) Department of Modern Physics, University of Science and Technology of China, Anhui; (c) Department of Physics, Nanjing University, Jiangsu; (d) School of Physics, Shandong University, Shandong, China
³⁴Laboratoire de Physique Corpusculaire, Clermont Université and Université Blaise Pascal and CNRS/IN2P3, Clermont-Ferrand, France
³⁵Nevis Laboratory, Columbia University, Irvington NY, United States of America
³⁶Niels Bohr Institute, University of Copenhagen, Kobenhavn, Denmark
³⁷(a) INFN Gruppo Collegato di Cosenza; (b) Dipartimento di Fisica, Università della Calabria, Arcavata di Rende, Italy
³⁸AGH University of Science and Technology, Faculty of Physics and Applied Computer Science, Krakow, Poland
³⁹The Henryk Niewodniczanski Institute of Nuclear Physics, Polish Academy of Sciences, Krakow, Poland
⁴⁰Physics Department, Southern Methodist University, Dallas TX, United States of America
⁴¹Physics Department, University of Texas at Dallas, Richardson TX, United States of America
⁴²DESY, Hamburg and Zeuthen, Germany
⁴³Institut für Experimentelle Physik IV, Technische Universität Dortmund, Dortmund, Germany
⁴⁴Institut für Kern- und Teilchenphysik, Technical University Dresden, Dresden, Germany
⁴⁵Department of Physics, Duke University, Durham NC, United States of America
⁴⁶SUPA - School of Physics and Astronomy, University of Edinburgh, Edinburgh, United Kingdom
⁴⁷INFN Laboratori Nazionali di Frascati, Frascati, Italy
⁴⁸Fakultät für Mathematik und Physik, Albert-Ludwigs-Universität, Freiburg, Germany
⁴⁹Section de Physique, Université de Genève, Geneva, Switzerland

- ^{50(a)}INFN Sezione di Genova; ^(b)Dipartimento di Fisica, Università di Genova, Genova, Italy
^{51(a)}E. Andronikashvili Institute of Physics, Tbilisi State University, Tbilisi; ^(b)High Energy Physics Institute, Tbilisi State University, Tbilisi, Georgia
⁵²II Physikalisch Institut, Justus-Liebig-Universität Giessen, Giessen, Germany
⁵³SUPA - School of Physics and Astronomy, University of Glasgow, Glasgow, United Kingdom
⁵⁴II Physikalisch Institut, Georg-August-Universität, Göttingen, Germany
⁵⁵Laboratoire de Physique Subatomique et de Cosmologie, Université Joseph Fourier and CNRS/IN2P3 and Institut National Polytechnique de Grenoble, Grenoble, France
⁵⁶Department of Physics, Hampton University, Hampton VA, United States of America
⁵⁷Laboratory for Particle Physics and Cosmology, Harvard University, Cambridge MA, United States of America
^{58(a)}Kirchhoff-Institut für Physik, Ruprecht-Karls-Universität Heidelberg, Heidelberg; ^(b)Physikalisches Institut, Ruprecht-Karls-Universität Heidelberg, Heidelberg; ^(c)ZITI Institut für technische Informatik, Ruprecht-Karls-Universität Heidelberg, Mannheim, Germany
⁵⁹Faculty of Applied Information Science, Hiroshima Institute of Technology, Hiroshima, Japan
⁶⁰Department of Physics, Indiana University, Bloomington IN, United States of America
⁶¹Institut für Astro- und Teilchenphysik, Leopold-Franzens-Universität, Innsbruck, Austria
⁶²University of Iowa, Iowa City IA, United States of America
⁶³Department of Physics and Astronomy, Iowa State University, Ames IA, United States of America
⁶⁴Joint Institute for Nuclear Research, JINR Dubna, Dubna, Russia
⁶⁵KEK, High Energy Accelerator Research Organization, Tsukuba, Japan
⁶⁶Graduate School of Science, Kobe University, Kobe, Japan
⁶⁷Faculty of Science, Kyoto University, Kyoto, Japan
⁶⁸Kyoto University of Education, Kyoto, Japan
⁶⁹Department of Physics, Kyushu University, Fukuoka, Japan
⁷⁰Instituto de Física La Plata, Universidad Nacional de La Plata and CONICET, La Plata, Argentina
⁷¹Physics Department, Lancaster University, Lancaster, United Kingdom
^{72(a)}INFN Sezione di Lecce; ^(b)Dipartimento di Matematica e Fisica, Università del Salento, Lecce, Italy
⁷³Oliver Lodge Laboratory, University of Liverpool, Liverpool, United Kingdom
⁷⁴Department of Physics, Jožef Stefan Institute and University of Ljubljana, Ljubljana, Slovenia
⁷⁵School of Physics and Astronomy, Queen Mary University of London, London, United Kingdom
⁷⁶Department of Physics, Royal Holloway University of London, Surrey, United Kingdom
⁷⁷Department of Physics and Astronomy, University College London, London, United Kingdom
⁷⁸Laboratoire de Physique Nucléaire et de Hautes Energies, UPMC and Université Paris-Diderot and CNRS/IN2P3, Paris, France
⁷⁹Fysiska institutionen, Lunds universitet, Lund, Sweden
⁸⁰Departamento de Fisica Teorica C-15, Universidad Autonoma de Madrid, Madrid, Spain
⁸¹Institut für Physik, Universität Mainz, Mainz, Germany
⁸²School of Physics and Astronomy, University of Manchester, Manchester, United Kingdom
⁸³CPPM, Aix-Marseille Université and CNRS/IN2P3, Marseille, France
⁸⁴Department of Physics, University of Massachusetts, Amherst MA, United States of America
⁸⁵Department of Physics, McGill University, Montreal QC, Canada
⁸⁶School of Physics, University of Melbourne, Victoria, Australia
⁸⁷Department of Physics, The University of Michigan, Ann Arbor MI, United States of America
⁸⁸Department of Physics and Astronomy, Michigan State University, East Lansing MI, United States of America
^{89(a)}INFN Sezione di Milano; ^(b)Dipartimento di Fisica, Università di Milano, Milano, Italy
⁹⁰B.I. Stepanov Institute of Physics, National Academy of Sciences of Belarus, Minsk, Republic of Belarus
⁹¹National Scientific and Educational Centre for Particle and High Energy Physics, Minsk, Republic of Belarus
⁹²Department of Physics, Massachusetts Institute of Technology, Cambridge MA, United States of America
⁹³Group of Particle Physics, University of Montreal, Montreal QC, Canada
⁹⁴PN. Lebedev Institute of Physics, Academy of Sciences, Moscow, Russia
⁹⁵Institute for Theoretical and Experimental Physics (ITEP), Moscow, Russia
⁹⁶Moscow Engineering and Physics Institute (MEPhI), Moscow, Russia
⁹⁷Skobeltsyn Institute of Nuclear Physics, Lomonosov Moscow State University, Moscow, Russia

- ⁹⁸Fakultät für Physik, Ludwig-Maximilians-Universität München, München, Germany
⁹⁹Max-Planck-Institut für Physik (Werner-Heisenberg-Institut), München, Germany
¹⁰⁰Nagasaki Institute of Applied Science, Nagasaki, Japan
¹⁰¹Graduate School of Science and Kobayashi-Maskawa Institute, Nagoya University, Nagoya, Japan
¹⁰²(a)INFN Sezione di Napoli; (b)Dipartimento di Scienze Fisiche, Università di Napoli, Napoli, Italy
¹⁰³Department of Physics and Astronomy, University of New Mexico, Albuquerque NM, United States of America
¹⁰⁴Institute for Mathematics, Astrophysics and Particle Physics, Radboud University Nijmegen/Nikhef, Nijmegen, Netherlands
¹⁰⁵Nikhef National Institute for Subatomic Physics and University of Amsterdam, Amsterdam, Netherlands
¹⁰⁶Department of Physics, Northern Illinois University, DeKalb IL, United States of America
¹⁰⁷Budker Institute of Nuclear Physics, SB RAS, Novosibirsk, Russia
¹⁰⁸Department of Physics, New York University, New York NY, United States of America
¹⁰⁹Ohio State University, Columbus OH, United States of America
¹¹⁰Faculty of Science, Okayama University, Okayama, Japan
¹¹¹Homer L. Dodge Department of Physics and Astronomy, University of Oklahoma, Norman OK, United States of America
¹¹²Department of Physics, Oklahoma State University, Stillwater OK, United States of America
¹¹³Palacký University, RCPTM, Olomouc, Czech Republic
¹¹⁴Center for High Energy Physics, University of Oregon, Eugene OR, United States of America
¹¹⁵LAL, Université Paris-Sud and CNRS/IN2P3, Orsay, France
¹¹⁶Graduate School of Science, Osaka University, Osaka, Japan
¹¹⁷Department of Physics, University of Oslo, Oslo, Norway
¹¹⁸Department of Physics, Oxford University, Oxford, United Kingdom
¹¹⁹(a)INFN Sezione di Pavia; (b)Dipartimento di Fisica, Università di Pavia, Pavia, Italy
¹²⁰Department of Physics, University of Pennsylvania, Philadelphia PA, United States of America
¹²¹Petersburg Nuclear Physics Institute, Gatchina, Russia
¹²²(a)INFN Sezione di Pisa; (b)Dipartimento di Fisica E. Fermi, Università di Pisa, Pisa, Italy
¹²³Department of Physics and Astronomy, University of Pittsburgh, Pittsburgh PA, United States of America
¹²⁴(a)Laboratorio de Instrumentacao e Fisica Experimental de Particulas - LIP, Lisboa, Portugal; (b)Departamento de Fisica Teorica y del Cosmos and CAFPE, Universidad de Granada, Granada, Spain
¹²⁵Institute of Physics, Academy of Sciences of the Czech Republic, Praha, Czech Republic
¹²⁶Faculty of Mathematics and Physics, Charles University in Prague, Praha, Czech Republic
¹²⁷Czech Technical University in Prague, Praha, Czech Republic
¹²⁸State Research Center Institute for High Energy Physics, Protvino, Russia
¹²⁹Particle Physics Department, Rutherford Appleton Laboratory, Didcot, United Kingdom
¹³⁰Physics Department, University of Regina, Regina SK, Canada
¹³¹Ritsumeikan University, Kusatsu, Shiga, Japan
¹³²(a)INFN Sezione di Roma I; (b)Dipartimento di Fisica, Università La Sapienza, Roma, Italy
¹³³(a)INFN Sezione di Roma Tor Vergata; (b)Dipartimento di Fisica, Università di Roma Tor Vergata, Roma, Italy
¹³⁴(a)INFN Sezione di Roma Tre; (b)Dipartimento di Fisica, Università Roma Tre, Roma, Italy
¹³⁵(a)Faculté des Sciences Ain Chock, Réseau Universitaire de Physique des Hautes Energies - Université Hassan II, Casablanca; (b)Centre National de l'Energie des Sciences Techniques Nucléaires, Rabat; (c)Faculté des Sciences Semlalia, Université Cadi Ayyad, LPHEA-Marrakech; (d)Faculté des Sciences, Université Mohamed Premier and LPTPM, Oujda; (e)Faculté des sciences, Université Mohammed V-Agdal, Rabat, Morocco
¹³⁶DSM/IRFU (Institut de Recherches sur les Lois Fondamentales de l'Univers), CEA Saclay (Commissariat a l'Energie Atomique), Gif-sur-Yvette, France
¹³⁷Santa Cruz Institute for Particle Physics, University of California Santa Cruz, Santa Cruz CA, United States of America
¹³⁸Department of Physics, University of Washington, Seattle WA, United States of America
¹³⁹Department of Physics and Astronomy, University of Sheffield, Sheffield, United Kingdom
¹⁴⁰Department of Physics, Shinshu University, Nagano, Japan
¹⁴¹Fachbereich Physik, Universität Siegen, Siegen, Germany
¹⁴²Department of Physics, Simon Fraser University, Burnaby BC, Canada
¹⁴³SLAC National Accelerator Laboratory, Stanford CA, United States of America

- ^{144(a)}Faculty of Mathematics, Physics & Informatics, Comenius University, Bratislava; ^(b)Department of Subnuclear Physics, Institute of Experimental Physics of the Slovak Academy of Sciences, Kosice, Slovak Republic
- ^{145(a)}Department of Physics, University of Johannesburg, Johannesburg; ^(b)School of Physics, University of the Witwatersrand, Johannesburg, South Africa
- ^{146(a)}Department of Physics, Stockholm University; ^(b)The Oskar Klein Centre, Stockholm, Sweden
- ¹⁴⁷Physics Department, Royal Institute of Technology, Stockholm, Sweden
- ¹⁴⁸Departments of Physics & Astronomy and Chemistry, Stony Brook University, Stony Brook NY, United States of America
- ¹⁴⁹Department of Physics and Astronomy, University of Sussex, Brighton, United Kingdom
- ¹⁵⁰School of Physics, University of Sydney, Sydney, Australia
- ¹⁵¹Institute of Physics, Academia Sinica, Taipei, Taiwan
- ¹⁵²Department of Physics, Technion: Israel Institute of Technology, Haifa, Israel
- ¹⁵³Raymond and Beverly Sackler School of Physics and Astronomy, Tel Aviv University, Tel Aviv, Israel
- ¹⁵⁴Department of Physics, Aristotle University of Thessaloniki, Thessaloniki, Greece
- ¹⁵⁵International Center for Elementary Particle Physics and Department of Physics, The University of Tokyo, Tokyo, Japan
- ¹⁵⁶Graduate School of Science and Technology, Tokyo Metropolitan University, Tokyo, Japan
- ¹⁵⁷Department of Physics, Tokyo Institute of Technology, Tokyo, Japan
- ¹⁵⁸Department of Physics, University of Toronto, Toronto ON, Canada
- ^{159(a)}TRIUMF, Vancouver BC; ^(b)Department of Physics and Astronomy, York University, Toronto ON, Canada
- ¹⁶⁰Faculty of Pure and Applied Sciences, University of Tsukuba, Tsukuba, Japan
- ¹⁶¹Department of Physics and Astronomy, Tufts University, Medford MA, United States of America
- ¹⁶²Centro de Investigaciones, Universidad Antonio Narino, Bogota, Colombia
- ¹⁶³Department of Physics and Astronomy, University of California Irvine, Irvine CA, United States of America
- ^{164(a)}INFN Gruppo Collegato di Udine, Udine; ^(b)ICTP, Trieste; ^(c)Dipartimento di Chimica, Fisica e Ambiente, Università di Udine, Udine, Italy
- ¹⁶⁵Department of Physics, University of Illinois, Urbana IL, United States of America
- ¹⁶⁶Department of Physics and Astronomy, University of Uppsala, Uppsala, Sweden
- ¹⁶⁷Instituto de Física Corpuscular (IFIC) and Departamento de Física Atómica, Molecular y Nuclear and Departamento de Ingeniería Electrónica and Instituto de Microelectrónica de Barcelona (IMB-CNM), University of Valencia and CSIC, Valencia, Spain
- ¹⁶⁸Department of Physics, University of British Columbia, Vancouver BC, Canada
- ¹⁶⁹Department of Physics and Astronomy, University of Victoria, Victoria BC, Canada
- ¹⁷⁰Department of Physics, University of Warwick, Coventry, United Kingdom
- ¹⁷¹Waseda University, Tokyo, Japan
- ¹⁷²Department of Particle Physics, The Weizmann Institute of Science, Rehovot, Israel
- ¹⁷³Department of Physics, University of Wisconsin, Madison WI, United States of America
- ¹⁷⁴Fakultät für Physik und Astronomie, Julius-Maximilians-Universität, Würzburg, Germany
- ¹⁷⁵Fachbereich C Physik, Bergische Universität Wuppertal, Wuppertal, Germany
- ¹⁷⁶Department of Physics, Yale University, New Haven CT, United States of America
- ¹⁷⁷Yerevan Physics Institute, Yerevan, Armenia
- ¹⁷⁸Centre de Calcul de l’Institut National de Physique Nucléaire et de Physique des Particules (IN2P3), Villeurbanne, France
- ^aAlso at Laboratorio de Instrumentacao e Fisica Experimental de Particulas - LIP, Lisboa, Portugal
- ^bAlso at Faculdade de Ciencias and CFNUL, Universidade de Lisboa, Lisboa, Portugal
- ^cAlso at Particle Physics Department, Rutherford Appleton Laboratory, Didcot, United Kingdom
- ^dAlso at TRIUMF, Vancouver BC, Canada
- ^eAlso at Department of Physics, California State University, Fresno CA, United States of America
- ^fAlso at Novosibirsk State University, Novosibirsk, Russia
- ^gAlso at Fermilab, Batavia IL, United States of America
- ^hAlso at Department of Physics, University of Coimbra, Coimbra, Portugal
- ⁱAlso at Department of Physics, UASLP, San Luis Potosi, Mexico
- ^jAlso at Università di Napoli Parthenope, Napoli, Italy
- ^kAlso at Institute of Particle Physics (IPP), Canada

¹Also at Department of Physics, Middle East Technical University, Ankara, Turkey

^mAlso at Louisiana Tech University, Ruston LA, United States of America

ⁿAlso at Dep Fisica and CEFITEC of Faculdade de Ciencias e Tecnologia, Universidade Nova de Lisboa, Caparica, Portugal

^oAlso at Department of Physics and Astronomy, University College London, London, United Kingdom

^pAlso at Group of Particle Physics, University of Montreal, Montreal QC, Canada

^qAlso at Department of Physics, University of Cape Town, Cape Town, South Africa

^rAlso at Institute of Physics, Azerbaijan Academy of Sciences, Baku, Azerbaijan

^sAlso at Institut für Experimentalphysik, Universität Hamburg, Hamburg, Germany

^tAlso at Manhattan College, New York NY, United States of America

^uAlso at School of Physics, Shandong University, Shandong, China

^vAlso at CPPM, Aix-Marseille Université and CNRS/IN2P3, Marseille, France

^wAlso at School of Physics and Engineering, Sun Yat-sen University, Guangzhou, China

^xAlso at Academia Sinica Grid Computing, Institute of Physics, Academia Sinica, Taipei, Taiwan

^yAlso at Dipartimento di Fisica, Università La Sapienza, Roma, Italy

^zAlso at DSM/IRFU (Institut de Recherches sur les Lois Fondamentales de l'Univers), CEA Saclay (Commissariat à l'Energie Atomique), Gif-sur-Yvette, France

^{aa}Also at Section de Physique, Université de Genève, Geneva, Switzerland

^{ab}Also at Departamento de Fisica, Universidade de Minho, Braga, Portugal

^{ac}Also at Department of Physics and Astronomy, University of South Carolina, Columbia SC, United States of America

^{ad}Also at Institute for Particle and Nuclear Physics, Wigner Research Centre for Physics, Budapest, Hungary

^{ae}Also at California Institute of Technology, Pasadena CA, United States of America

^{af}Also at Institute of Physics, Jagiellonian University, Krakow, Poland

^{ag}Also at LAL, Université Paris-Sud and CNRS/IN2P3, Orsay, France

^{ah}Also at Nevis Laboratory, Columbia University, Irvington NY, United States of America

^{ai}Also at Department of Physics and Astronomy, University of Sheffield, Sheffield, United Kingdom

^{aj}Also at Department of Physics, Oxford University, Oxford, United Kingdom

^{ak}Also at Institute of Physics, Academia Sinica, Taipei, Taiwan

^{al}Also at Department of Physics, The University of Michigan, Ann Arbor MI, United States of America

^{am}Also at Discipline of Physics, University of KwaZulu-Natal, Durban, South Africa

*Deceased